

# Testing the Dark Matter Hypothesis with Low Surface Brightness Galaxies and Other Evidence

Stacy S. McGaugh<sup>1</sup>

Department of Terrestrial Magnetism  
Carnegie Institution of Washington  
5241 Broad Branch Road, NW  
Washington, DC 20015

and

W. J. G. de Blok<sup>2</sup>

Kapteyn Astronomical Institute  
Postbus 800  
9700 AV Groningen  
The Netherlands

## ABSTRACT

The severity of the mass discrepancy in spiral galaxies is strongly correlated with the central surface brightness of the disk. Progressively lower surface brightness galaxies have ever larger mass discrepancies. No other parameter (luminosity, size, velocity, morphology) is so well correlated with the magnitude of the mass deficit.

The rotation curves of low surface brightness disks thus provide a unique data set with which to probe the dark matter distribution in galaxies. The mass discrepancy is apparent from  $R = 0$  giving a nearly direct map of the halo mass distribution. The luminous mass is insignificant.

Interpreting the data in terms of dark matter leads to troublesome fine-tuning problems. Different observations require contradictory amounts of dark matter. Structure formation theories are as yet far from able to explain the observations.

*Subject headings:* cosmology: dark matter — galaxies: formation — galaxies: halos — galaxies: kinematics and dynamics — galaxies: structure — gravitation

What gets us into trouble is not what we don't know.

It's what we know for sure that just aint so.

— Yogi Berra

---

<sup>1</sup>Present Address: Physics and Astronomy, Rutgers University, 136 Frelinghuysen Road, Piscataway, NJ 08854-8019

<sup>2</sup>Present Address: Astrophysics Groups, School of Physics, University of Melbourne, Parkville, Victoria 3052, Australia

## 1. The Problem

The evidence for the existence of dark matter is clear in a great variety of data (Trimble 1987). These include the Oort discrepancy in the disk of the Milky Way (Kuijken & Gilmore 1989; Bahcall et al. 1992), the velocity dispersions of dwarf Spheroidal galaxies (e.g., Vogt et al. 1995), the flat rotation curves of spiral galaxies (Rubin et al. 1980; Bosma 1981), the statistics of satellite galaxy orbits (Zaritsky & White 1994), the timing argument in the Local Group (Kahn & Woltjer 1959), the velocity dispersions of clusters of galaxies (Zwicky & Humason 1964), bulk flows on large scales (Lynden-Bell et al. 1988; Mould et al. 1993), the excess of mass density in the universe over that in visible in galaxies ( $\Omega_{dyn} \gg \Omega_{gal}$ ; Ostriker & Steinhardt 1995), and gravitational lensing (Tyson et al. 1990).

What these data really demonstrate is that the observed distribution of luminous matter together with the usual dynamical equations can not reproduce the observations. This can be interpreted *either* to require dark matter, *or* as a need to modify the equations we use (e.g., the law of gravity). In this series of papers we examine and compare the pros and cons of both alternatives. Here we shall examine the dark matter hypothesis. In companion papers [McGaugh & de Blok 1998 (paper II); de Blok & McGaugh 1998 (paper III)], we examine alternative dynamical theories.

The H I rotation curves of disk galaxies provide powerful tests of the various hypotheses (e.g., Kent 1987; Begeman et al. 1991). These share the general characteristic of becoming asymptotically *flat* at large radii. One would expect  $V(R) \propto R^{-1/2}$  without dark matter.

The major advantage of using H I rotation curves is that the geometry of the orbits is obvious. Dissipation in the gas enforces circular orbits. Thus it is possible to directly equate the centripetal acceleration

$$a_c = \frac{V^2}{R} \tag{1}$$

with the gravitational acceleration

$$g_N = -\frac{\partial\varphi}{\partial R} \tag{2}$$

determined from the Poisson equation

$$\nabla^2\varphi = 4\pi G\rho \tag{3}$$

in order to predict the expected form of the rotation curve  $V(R)$  from any given mass distribution  $\rho(R)$ . In no other type of system are tests so direct and free of assumptions.

An important aspect of any test is probing a large dynamic range in the relevant parameters. It turns out that the luminous surface density of disks is a critical parameter (see §4). So the important thing is to have a large dynamic range in surface brightness. This is exemplified by the fact that the few good rotation curves of low surface brightness dwarf galaxies which exist are constantly being reanalyzed (e.g., Flores & Primack 1994; Moore 1994) precisely because they

provide leverage for testing ideas principally motivated by data for high surface brightness (HSB) spirals. Here, we augment existing data with our own data for low surface brightness (LSB) disk galaxies (van der Hulst et al. 1993; de Blok et al. 1996) to probe the lower extremes of surface brightness with many more galaxies than previously available thus extending the dynamic range in the critical parameter of luminous surface density.

One important result is the universality of the Tully-Fisher relation across this increased dynamic range in surface brightness (Zwaan et al. 1995; Sprayberry et al. 1995). This requires a surprising fine-tuning between the optical properties (central surface brightness) of a galaxy and its halo (mass-to-light ratio). Zwaan et al. (1995) suggested that galaxies must become progressively more dark matter dominated towards lower surface brightnesses. This conclusion was confirmed by H I rotation curves (de Blok et al. 1996) which require a greater ratio of dark to luminous mass at any given radius in LSB relative to HSB galaxies (de Blok & McGaugh 1997). Another essential result is the way in which the shape of rotation curves changes systematically with surface brightness from steeply rising curves in HSB galaxies to slowly rising curves in LSB galaxies.

The challenge is to fit these and other observations into a consistent and coherent picture of the formation and evolution of dark matter halos and their associated spiral disks. In this paper we examine the difficulties encountered in undertaking this task. As yet, it is impossible to develop such a picture without resorting to a large number of fine-tuned relations between supposedly independent galaxy properties.

In section 2, we describe the data. In section 3, we define symbols and clarify terms. Section 4 gives a summary of the most relevant empirical facts. The physical interpretation of the Tully-Fisher relation is discussed in §5. In §6 we introduce and test a variety of galaxy formation models. Section 7 tests various dark matter candidates and §8 discusses the implications of baryon fractions determined from a variety of data.

We adopt a Hubble constant of  $H_0 = 75 \text{ kms}^{-1}\text{Mpc}^{-1}$  throughout.

## 2. Data

We employ data we have obtained for low surface brightness disk galaxies in the 21 cm line as described in van der Hulst et al. (1993) and de Blok et al. (1996), combined with optical surface photometry presented in those papers and in McGaugh & Bothun (1994) and de Blok et al. (1995). We augment our own data with published data for dwarfs and high surface brightness spirals for which both 21 cm rotation curves and adequate surface photometry are available, as compiled by Broeils (1992) and de Blok et al. (1996).

The data are listed in Table 1. The line demarcates our own data from that drawn from the literature. The columns give (1) the name of the galaxy, (2) its  $B$ -band absolute magnitude  $M_B$ ,

(3) the inclination corrected central surface brightness  $\mu_0$  the disk in  $B$  mag arcsec $^{-2}$ , (4) the scale length of the disk  $h$  in kpc, (5) the circular velocity  $V_c$  in the flat part of the rotation curve, (6) the inclination  $i$  in degrees, and (7) the dynamical mass to light ratio  $\Upsilon_o$  measured at  $R = 4h$  in  $\mathcal{M}_\odot/L_\odot$  (see §3).

A requirement for inclusion in Table 1 is that both an H I rotation curve and surface photometry exist. Most data of the latter sort are in  $B$  so we use that as standard. Though  $R$  or even  $K$  might seem preferable, this severely reduces the amount of available data. The choice of bandpass makes no difference to the interpretation. In collecting data from the literature, we have attempted to be as inclusive as possible, in some cases transforming photographic surface photometry from different bands to  $B$  when a color is available.

We correct optical surface brightnesses to face-on values assuming that the disk is optically thin. This is supported by statistical studies which show that spiral galaxies are semi-transparent throughout their disks, except for the innermost regions (e.g., Huizinga & van Albada 1992; Giovanelli et al. 1994). In general the outer parts of galaxies are optically thin. Measurements of extinction in foreground spirals obscuring a background galaxy suggest extinction values of  $\sim 0.3$  mag in  $B$  in the interarm regions of the outer parts of a spiral (Andredakis & van der Kruit 1992; White & Keel 1992). As  $\mu_0$  is not a measure of the actual surface brightness in the center of a galaxy, but the intercept of a fit to the disk profile which depends more on the outer than the inner points, extinction is not a serious concern. This is especially true in LSB galaxies where the metallicity and dust content are low (McGaugh 1994). The assumption of optically thin disks is only likely to be invalid in edge-on galaxies.

Bulges have little effect on the derived  $\mu_0$  of LSB galaxies (McGaugh & Bothun 1994; de Blok 1995; see also de Jong 1996a; Courteau 1996). A bigger problem is the great inhomogeneity of sources of the surface photometry amongst the literature data. However, the range is surface brightness in our sample ( $\sim 5$  mag arcsec $^{-2}$ ) is much larger than the most pessimistic error estimates on the surface brightnesses.

Sometimes, the rotation curves themselves are lacking. For completeness, we published all our synthesis data in de Blok et al. (1996), but not all galaxies are useful for dynamical analyses (Table 2). We observed galaxies of a variety of inclinations, and some are too face-on to be of use here. We nonetheless prefer to accept large errors than to arbitrarily limit the data, and so impose a very liberal inclination limit:  $i > 25^\circ$ .

As well as very face-on galaxies, there are LSB galaxies with such slowly rising rotation curves that even the synthesis observations do not reach the flat portion of the rotation curve. In others, substantial asymmetries are present. This is not an uncommon feature of galaxies generally (Richter & Sancisi 1994), and calls into question the assumption of circular orbits on which dynamical analyses are based. Hence these galaxies are also excluded.

The list of excluded galaxies in Table 2 is not precisely identical to that for our rotation curve fits (de Blok & McGaugh 1997; paper III) because that is a different sort of analysis. The

fits depend to a large extent on the shape of the rotation curve which can be sensitive to the resolution of the observations. In this analysis we are only concerned with the amplitude  $V_c$  of the rotation curve so we can proceed if  $V_c$  is reasonably well defined.

Some tests are less sensitive to these limitations than others, so it will sometimes be possible to make use of the galaxies in Table 2. However, unless so noted, the sample is restricted to those galaxies listed in Table 1. This sample is not complete in any volume-limited sense, but that is not the goal of this work. Our aim here is to represent as broad as possible a range of the relevant physical parameters. The collected data span a factor of 4000 in luminosity, 30 in size, and nearly 100 in surface brightness. This large dynamic range in surface brightness with good sampling of the LSB regime is the essence of the new contribution of this work.

### 3. Definitions

Here we explicitly define the symbols and notation we will use. The optical luminosity of a galaxy will be denoted in the usual way by  $L_O$  and the corresponding absolute magnitude by  $M_O$ , where  $O$  denotes the relevant band pass. Unless otherwise specified, all optical quantities are  $B$ -band measurements. To symbolically distinguish between absolute magnitude and mass, the latter will be denoted by  $\mathcal{M}$ .

The light distribution of an exponential disk is characterized by the central surface brightness  $\mu_0$  and the scale length  $h$  (de Vaucouleurs 1959). As the intercept and slope of a fit to the light profile, these describe the global luminous surface density and size of disks. It is sometimes convenient to discuss surface brightness in  $\text{mag arcsec}^{-2}$ , and sometimes in linear units  $L_\odot \text{pc}^{-2}$ . In general, we will use  $\mu$  to specify a surface brightness,  $\Sigma$  to specify a luminous surface density, and  $\sigma$  to specify a mass surface density. The total luminosity of the disk component is of course simply related to the disk parameters by  $L = 2\pi\Sigma_0 h^2$ .

An important quantity is the mass to light ratio, which we will denote by  $\Upsilon$ . We need to distinguish several different mass to light ratios:

1.  $\Upsilon_T$ , the total mass to light ratio,
2.  $\Upsilon_o$ , the observable dynamical mass to light ratio, and
3.  $\Upsilon_*$ , the mass to light ratio of the stars.

The latter relates stellar mass to observable luminosity; it includes any remnants that occur in the natural course of stellar evolution (e.g., white dwarfs) but not baryons in the gas phase. The total mass to light ratio  $\Upsilon_T$  includes all mass, and encompasses the entirety of any halo. Since  $\mathcal{M} \propto R$  for a flat rotation curve, and there exists no clear evidence of an edge to any halo mass distribution,  $\Upsilon_T$  is a purely theoretical construct. It is nonetheless useful to keep in mind when

discussing the observable mass to light ratio  $\Upsilon_o$ . This includes all mass (including dark matter) within some finite observable radius  $R_o$ . For the usual assumption of sphericity, the mass within  $R_o$  is

$$\mathcal{M}(R_o) = R_o V^2(R_o)/G. \quad (4)$$

Deviations from sphericity can complicate this equation, but only by geometrical factors. They do not alter the basic functional dependence which is the issue of relevance here.

The value of  $G$  is known and  $L$ ,  $R$  and  $V$  are directly measured. The quantities  $\mathcal{M}(R_o)$  and  $\Upsilon_o$  are thus uniquely determined by equation (4). If  $\Upsilon_o$  exceeds what is reasonable for  $\Upsilon_*$ , we infer the presence of dark matter.

The absolute mass inferred depends on the distance scale which enters through  $R$  ( $V$  is distance independent for the redshifts that concern us). The choice of  $H_0$  is not important to the shape derived for trends of  $\Upsilon_o$  with optical properties. The absolute value of  $\Upsilon_o$  will of course shift with changes to the distance scale.

The choice of  $R_o$  is important. It is tempting simply to take this as the largest radius measured. However, this depends more on the details of the observations than anything intrinsic to a galaxy. It is therefore necessary to make a sensible choice for  $R_o$  which can systematically be applied to all disk galaxies. Since  $V(R) \rightarrow V_c$  as  $R$  becomes large, one obvious stipulation is that  $R_o$  be sufficiently large that the rotation curves have become essentially flat. The rotation curves of LSB galaxies are observed to rise slowly (de Blok et al. 1996), and in some cases the flat portion has not yet been reached at the last measured point. These galaxies must be excluded from analysis. In most cases, the rotation curves are still rising slightly but becoming asymptotically flat. We proceed if the gradient in the outer slope is small (following Broeils 1992; see Fig. 11 of de Blok et al. 1996). The actual observed value is used, not the apparent asymptotic value. Another stipulation in defining  $R_o$  is that it contain essentially all of the luminosity of the galaxy, so that  $\Upsilon_o$  has the obvious meaning. A further requirement is that  $R_o$  not be so large as to exceed the last measured point of the observations.

Ideally, we would like to relate  $R_o$  to the extent of the mass distribution. Presumably dark halos have some sort of edge, which we will denote by  $R_H$ . Since we can not see the dark matter, it is impossible to relate  $R_o$  to  $R_H$  without somehow assuming the answer. Observations are incapable of uniquely deconvolving the contribution of luminous and dark mass into any useful scale radius (e.g., van Albada & Sancisi 1986; Lake & Feinswog 1989; de Blok & McGaugh 1997).

The only fair measure of a disk's size observationally available is the scale length  $h$ . Isophotal radii like  $R_{25}$  are meaningless for LSB galaxies: the dimmest objects studied here have  $\mu_0 \approx 25$ , so  $R_{25} \approx 0$  by definition. The effective (half light) radius is proportional to the scale length for pure disk systems, but depends on the bulge component in general. We are concerned here with defining a radius for the rotating disk, so the scale length is preferable to the effective radius.

It might seem preferable to define a half mass radius of the observable matter by combining

stars and gas. However, this requires that molecular gas be mapped as well as the H I and optical light. Even if such data were available, some assumption about  $\Upsilon_*$  and the  $CO/H_2$  conversion factor would still have to be made.

We therefore choose to define  $R_o$  in units of  $h$ , in particular  $R_o = 4h$ . Most rotation curves have reached their asymptotic velocities by 3 scale lengths, while the last measured point for the bulk of the data is around  $5h$ . Four scale lengths contains 91% of the luminosity of a pure exponential disk extrapolated to infinity, and disks are generally thought to truncate around 4 or 5 scale lengths (van der Kruit 1987). A choice of  $5h$ , or any other definition based on the disk light distribution, simply inserts a multiplicative factor.

As a matter of nomenclature, we will refer to the observable gas and stars as “baryonic” matter, and treat the dark matter as a distinct component of unknown composition.

#### 4. Observational Facts

Empirical results about the rotation curves and what they imply for the dependence of the mass discrepancy on the optical properties of galaxies can be summarized independently of any theoretical framework by the following four facts:

1. All disk galaxies obey the same Tully-Fisher relation, irrespective of surface brightness or band pass (Fig. 1; Sprayberry et al. 1995; Zwaan et al. 1995; Hoffman et al. 1996; Tully & Verheijen 1997).
2. At a given luminosity, the shape of rotation curves  $V(R)$  varies systematically with surface brightness (Fig. 2). When  $R$  is measured in physical units (kpc), lower surface brightness galaxies have rotation curves which rise more gradually. When  $R$  is measured in terms of disk scale lengths, the shape of  $V(R/h)$  is more similar though not necessarily identical (see Fig. 8 of de Blok et al. 1996).
3. The mass discrepancy manifests itself at progressively smaller radii in dimmer galaxies (de Blok & McGaugh 1996, 1997; Fig. 3; see also Casertano & van Gorkom 1991; Broeils 1992; van Zee et al. 1997).
4. The severity of the mass discrepancy is strongly correlated with the central surface brightness of the disk (Fig. 4; de Blok et al. 1996). This is the  $\Upsilon$ - $\Sigma$  relation (Zwaan et al. 1995).

##### 4.1. Fact 1

The relationship between luminosity and linewidth has long been known (Tully & Fisher 1977). That the same relation holds for all surface brightnesses has been obtained independently

by Sprayberry et al. (1995), Zwaan et al. (1995), Hoffman et al. 1996, and Tully & Verheijen 1997. These different works all obtain the same observational result but offer varying interpretations of it.

The interpretation depends entirely on the basic assumptions one must make. One obvious assumption is that light traces mass, in which case LSB galaxies should rotate slowly for their luminosity and *not* obey the Tully-Fisher relation. This occurs because  $R$  is larger for the same  $L$ , reducing  $V$  in equation (4) (Zwaan et al. 1995). That LSB galaxies are not expected to fall on the Tully-Fisher relation was first discussed by Aaronson et al. (1979) and Romanishin et al. (1982) using this assumption. Other assumptions can also be made (discussed in detail §5) but generally result in some sort of shift of LSB galaxies off the Tully-Fisher relation (e.g., Dalcanton et al. 1995). The only scenario in which no shift is expected is one in which halos of a given mass are identical. This assumption is itself motivated by the Tully-Fisher relation, so it offers no independent expectation value. In cases where there is a clear expectation of a shift, that expectation is not realized.

Indeed, it is already difficult to understand a luminosity-linewidth relation with little scatter. One expects a great deal more scatter for plausible initial conditions (e.g., Eisenstein & Loeb 1995). The lack of surface brightness segregation in the luminosity-linewidth plane complicates things much further (as discussed in §5). For now, note that in Fig. 1 a Tully-Fisher relation is obtained for both  $W_{20}^c$  and  $V_c$ : the velocity width is as expected an indicator of the rotation velocity. The scatter is greater when the linewidth is used (0.9 vs. 0.6 mag.). We can not say much about the intrinsic scatter of the Tully-Fisher relation since we include low inclination galaxies. This naturally increases the scatter, so the intrinsic scatter is presumably smaller than what we measure. The slopes obtained from Fig 1(a) and (b) are marginally different, being  $-7 \pm 2$  in (a) and  $-9.4 \pm 1$  in (b). This may indicate that  $W_{20}^c$  is not a perfect indicator of the real quantity of interest,  $V_c$ .

The most important fact is that there is a strong luminosity-rotation velocity relation with little intrinsic scatter and a slope indistinguishable from the theoretical value. The details of the band-pass dependence of the slope are not critical (see Appendix) as we are not trying to establish a calibration of the Tully-Fisher relation, but rather trying to understand why LSB galaxies follow it at all. In this context, we are concerned with the relation of stellar *mass* to the flat rotation velocity  $V_c$ . The near infrared is thought to be the best indicator of stellar mass, and both  $H$  (Aaronson et al. 1979) and  $K$  (Tully & Verheijen 1997) band Tully-Fisher relations have slopes indistinguishable from the theoretical expectation  $-10$ .

## 4.2. Fact 2

It is well known that the shape of galaxy rotation curves is luminosity dependent (Burstein et al. 1982; Persic et al. 1996). At a given luminosity, the shape varies systematically with surface



brightness in that the rotation curves of LSB galaxies rise more gradually than do those of high surface brightness galaxies. This behavior *is* expected if light traces mass and surface mass density follows from surface brightness in the obvious way. This is indeed the case at small radii, both for the specific example illustrated in Fig. 2 (de Blok & McGaugh 1996a) and in general. Moreover, the relative similarity of  $V(R/h)$  suggests that the dark halo is strongly coupled to the properties of the disk (see also paper II).

If surface brightness is a good indicator of mass density, LSB galaxies should not lie on the Tully-Fisher relation. Yet they do. Reconciling facts (1) and (2) proves to be very difficult, and leads to fact (3).

### 4.3. Fact 3

In high surface brightness spiral galaxies, it is generally possible to attribute essentially all of the observed rotation to the luminous disk out to 3 scale lengths or so by scaling the disk contribution up to the maximum value allowed by the amplitude of the inner part of the rotation curve (Bosma 1981; Kent 1987; Sancisi & van Albada 1987; Sanders 1990). This “maximum disk” solution has led to a general picture in which the luminous material dominates the inner part of spiral galaxies, and dark matter only becomes dominant in the outer fringes near the edge of the luminous disk. An important aspect of this picture is that the peak in the rotation curve of the exponential disk at  $R = 2.2h$  is comparable in amplitude to the circular velocity due to the halo [ $V_{disk}^{peak}(2.2h) \approx V_H$ ], giving a smooth transition between the two components (the disk-halo “conspiracy”).

The disks of LSB spirals can not be maximal in this sense. Because they are very diffuse, the Newtonian rotation curves of LSB disks peak at very low amplitudes ( $\ll V_c$ ) for plausible values of the mass to light ratio of the stellar population. From a purely dynamical standpoint, there is some room to consider values of  $\Upsilon_*$  which are unreasonably large for the blue stellar populations of LSB galaxies. However, even for  $\Upsilon_* \sim 10$  (as opposed to reasonable values of  $\sim 1$  or  $2$ ), it is still not possible to attribute a velocity comparable to  $V_c$  to the disk. Even larger  $\Upsilon_*$  are not allowed by the slow rate of rise of the rotation curves. The disk simply can not dominate in these galaxies except at very small radii: the mass discrepancy sets in at essentially  $R = 0$  (Fig. 3). Only the highest surface brightness disks can be maximal in the sense that luminous disks dominates the inner dynamics, with dark matter only becoming important at large radii. There is no reason to believe that a segregation between inner dominance by a disk and outer dominance by a dark matter halo is a general property of galaxies.

#### 4.4. Fact 4

The severity of the global mass discrepancy, as measured by the observed mass to light ratio  $\Upsilon_o$ , is correlated with both luminosity and surface brightness (Fig. 4). It is not correlated with the optical size of the galaxy. The correlation with surface brightness is much stronger ( $\mathcal{R} = 0.88$ ) than with absolute magnitude ( $\mathcal{R} = 0.46$ ). The scatter in the former case can plausibly be attributed entirely to observational error, especially considering the very inhomogeneous sources of the surface photometry. In the case of  $M_B$  there is substantial real scatter. Absolute magnitude and surface brightness are themselves weakly correlated ( $\mathcal{R} = 0.50$  in this sample), so it seems likely that the relation between luminosity and  $\Upsilon_o$  is due to the convolution of the strong  $\Upsilon_o$ - $\Sigma_0$  relation with the lack of a size relation through  $L \propto \Sigma_0 h^2$ . Surface brightness, not luminosity or morphological type, is the variable of greatest interest.

### 5. The Tully-Fisher and $\Upsilon_o$ - $\Sigma$ Relations

The relation between  $\Upsilon_o$  and  $\mu_0$  can be derived from the Tully-Fisher relation (Zwaan et al. 1995) assuming that the observed velocity width  $W$  is proportional to the asymptotic rotation velocity  $V_c$ , and taking  $R \propto \sqrt{L/\Sigma}$ . The latter is true by definition; the former is empirically confirmed by the full rotation curve data. Various authors (i.e., Sprayberry et al. 1995; Salpeter & Hoffman 1996) give apparently conflicting results, but these stem entirely from differing definitions of  $R_o$ . The *data* are all consistent.

To discuss possible interpretations of the Tully-Fisher relation, we make the usual assumptions that the H I gas is in circular orbit ( $a_c = V^2(R)/R$ ) and that halos are spherical and dominant where  $V(R) \rightarrow V_c$  so that  $g_N = GM(R)/R^2$ . Setting  $a_c = g_N$  gives

$$V^2(R) = \frac{GM(R)}{R}. \quad (5)$$

These are very basic assumptions which are widely employed; plausible deviations (e.g., triaxial halos) will not alter the gist of the results. Observationally, the Tully-Fisher relation is

$$L_j \propto V_c^{x_j} \quad (6)$$

where  $x_j$  is the slope in band pass  $j$ . To relate equation (5) to (6), let us define a mass surface density

$$\sigma(R) \equiv \frac{\mathcal{M}(R)}{R^2} \quad (7)$$

and make a substitution of variables so that

$$V^4 = \frac{G^2 \mathcal{M}^2(R)}{R^2} = G^2 \sigma \mathcal{M}(\sigma). \quad (8)$$

By definition,  $\mathcal{M}(R) = \Upsilon_j(R)L_j$  and  $\sigma(R) = \Upsilon_j(R)\Sigma_j(R)$ . Here,  $\Sigma_j(R)$  is the average surface brightness within  $R$  (which will decrease as  $R$  grows) and  $\Upsilon_j(R)$  is the dynamical mass to light

ratio within radius  $R$ . Both  $\Sigma_j$  and  $\Upsilon_j$  are strong functions of  $R$ . However, we are concerned only with the relative functional dependencies, so the actual value of  $R$  drops out where  $V(R) = V_c$ .

In theory,

$$V_c^4 \propto \Upsilon_j^2 \Sigma_j L_j, \quad (9)$$

while in actuality

$$V_c^{x_j} \propto L_j. \quad (10)$$

As discussed by Zwaan et al. (1995), one needs to arrange to keep the term  $\Upsilon_j^2 \Sigma_j$  constant in order to recover the observed Tully-Fisher relation from basic physics. This is often attributed to a universal constancy of the mass to light ratio and Freeman’s law (Freeman 1970) which states that all spirals have essentially the same surface brightness,  $\mu_0 \approx 21.65$  mag arcsec $^{-2}$ . By definition LSB galaxies deviate from this value, and *should not* fall on the same Tully-Fisher relation as Freeman disks if the mass to light ratio is constant as generally assumed. Fig. 5 shows the relation expected from equation (9) if  $\Upsilon_o$  is constant; the range of surface brightnesses examined is large enough that this effect would be very readily apparent. Instead of following this relation, LSB galaxies rigorously adhere to *the* Tully-Fisher relation. The mass to light ratio must somehow be fine tuned to compensate.

Consider the error budget required. In magnitude units, the Tully-Fisher relation is  $M_j = -10 \log V_c + C$  assuming  $x_j = 4$ . Hence

$$\delta M = 4.34 \frac{\delta V_c}{V_c}, \quad (11)$$

so an intrinsic scatter of  $< 0.6$  mag. stems from a modest  $< 14\%$  intrinsic variation in  $V_c$ . Disk and halo must combine to specify  $V_c$  very precisely. More generally, the variation is

$$|\delta M|^2 = |\delta \mu_0|^2 + 18.86 \left| \frac{\delta V_c}{V_c} \right|^2 + 1.18 \left| \frac{\delta \Upsilon}{\Upsilon} \right|^2. \quad (12)$$

A one magnitude shift in  $\mu_0$  should translate directly into one magnitude in  $M$ . Even for disks which obey the Freeman (1970) Law, the scatter in  $\mu_0$  (0.35 mag.) should propagate directly into the Tully-Fisher relation. Here we have disks spanning nearly 5 magnitudes in  $\mu_0$ . The mass to light ratio must be fine tuned to compensate, with essentially zero scatter.

## 5.1. Implications

The observed mass to light ratio  $\Upsilon_o$  as we have defined it includes all mass within some arbitrary radius  $R_o$ . The exact definition of  $R_o$  is not essential, as long as we choose a fixed number of scale lengths which encompasses the luminous matter and reaches the flat part of the rotation curve. Then, using equation (9),

$$\Upsilon_o = \frac{\lambda \Upsilon_*}{f_b f_*} \propto \Sigma^{-1/2} \quad (13)$$

where  $\Upsilon_*$  is the mass to light ratio of the stellar population,  $f_b = \mathcal{M}_b/\mathcal{M}_T$  is the baryonic mass fraction,  $f_* = \mathcal{M}_*/\mathcal{M}_b$  is the fraction of baryonic disk mass in the form of stars, and  $\lambda = \mathcal{M}(R_o)/\mathcal{M}_T$  is the fraction of the total mass encompassed by the edge of the disk. Note that since  $\mathcal{M} \propto R$ ,  $\lambda \approx R_o/R_H$  where  $R_H$  is the halo radius (edge). We thus decompose  $\Upsilon_o$  into four fundamental parameters; two involve galaxy evolution ( $\Upsilon_*$ ,  $f_*$ ) and two involve galaxy formation ( $f_b$ ,  $\lambda$ ). The requirement  $\Upsilon_o \propto \Sigma^{-1/2}$  now implies that a combination of four parameters must be fine tuned with surface brightness. Let us examine each of them in turn.

## 5.2. Evolution

Zwaan et al. (1995) attributed the observed adherence to the Tully-Fisher relation to evolutionary regulation. From a theoretical perspective, not taking the surface brightness effects into account, Eisenstein & Loeb (1995) came to the same conclusion in more general terms. They showed that it was very difficult to obtain a Tully-Fisher relation with the small observed scatter from plausible initial conditions. There should always be some scatter in the density structure of halos so that velocity is not so precisely specified by total mass and luminosity. Some evolutionary regularizing effects must thus reduce the scatter. The physical mechanism by which this occurs is unknown. Feedback from star formation activity is often invoked, but it is hard to see how the stochastic energy input of massive stars will have a strong *regularizing* effect. Since the nature of the evolutionary regulation is unclear, let us simply examine the consequences for  $\Upsilon_*$  and  $f_*$ .

### 5.2.1. Stellar Mass to Light Ratios

The mass to light ratio of a stellar population is measured directly in our own Milky Way, where  $\Upsilon_* \approx 1.7$  in  $B$  (Kuijken & Gilmore 1989). This appears to be typical of high surface brightness disks, with substantial variation and uncertainty. Bottema (1997) finds  $\Upsilon_* = 1.8 \pm 0.5$  from velocity dispersions. For LSB galaxies, one infers slightly smaller  $\Upsilon_*$  from their colors,  $\sim 1$  with great uncertainty (McGaugh & Bothun 1994; de Blok et al. 1995). There is a lot of real scatter in color at any given surface brightness, implying substantial scatter in  $\Upsilon_*$ .

The inferred trend of  $\Upsilon_*$  with  $\Sigma_0$  is much smaller in magnitude than the  $\Upsilon_o$ - $\Sigma_0$  relation and has the opposite sign. In addition to what the colors imply for  $\Upsilon_*$ , the slow rate of rise of the rotation curves (de Blok & McGaugh 1996 1997) dynamically rules out the large  $\Upsilon_*$  values that are needed in LSB galaxies to explain the  $\Upsilon_o$ - $\Sigma_0$  relation. The peak amplitudes of the rotation curves of the stellar disk are much smaller than  $V_c$  so the stellar disks alone cannot cause the TF relation, let alone the  $\Upsilon_o$ - $\Sigma_0$  fine-tuning. The only way to alter this conclusion is to drop the usual assumption that light traces *stellar* mass, and make  $\Upsilon_*$  a strong function of radius [the unlikely form  $\Upsilon_* \propto R^{-1} \exp(R/h)$  would be required]. It is therefore unlikely that the  $\Upsilon_o$ - $\Sigma_0$  relation can be caused by a  $\Upsilon_*$ - $\Sigma_0$  relation.

### 5.2.2. Stellar Mass Fractions

The fraction of the baryonic disk mass which is in the form of stars  $f_*$  is well correlated with surface brightness (Fig. 6; McGaugh & de Blok 1997). The correlation goes in the correct sense, with LSB galaxies having relatively fewer stars. The slope is approximately correct, though the correlation is not as tight as that with  $\Upsilon_o$ .

It is therefore tempting to attribute the fact that  $\Upsilon_o \propto \Sigma_0^{-1/2}$  to  $f_* \propto \Sigma_0^{1/2}$ . This would mean a regulatory mechanism which somehow maintains a mass fraction of stars appropriate to both the Tully-Fisher and  $\Upsilon_o$ - $\Sigma_0$  relations. It is possible to check this since the gas mass is directly measurable from the 21 cm flux. That is,  $\mathcal{M}_{gas} = \eta \mathcal{M}_{HI}$ , where  $\eta = 1.4$  is appropriate for solar metallicity atomic gas. Molecular gas does not seem to be common in LSB galaxies (Schombert et al. 1990) and is presumably distributed like the stars. If this is the case, it is subject to the same dynamical constraints as  $\Upsilon_*$ . Moreover, the approach to evolutionary regulation taken here is motivated by the similarity of the  $\Upsilon_o$ - $\Sigma_0$  and  $\mathcal{M}(HI)/L$ - $\Sigma_0$  relations. This motivation would vanish if molecular gas were more important than the H I.

We can correct  $\Upsilon_o$  for the atomic gas simply by subtracting its mass from the total. This removes the term  $f_*$  from equation (13):

$$\Upsilon_o^c = \frac{\mathcal{M}(R_o) - \mathcal{M}_{gas}}{L} = \frac{\lambda \Upsilon_*}{f_b}. \quad (14)$$

Though this accounts for the  $\mathcal{M}(HI)/L$ - $\Sigma_0$  relation, it makes no real difference to the  $\Upsilon_o$ - $\Sigma_0$  problem (Fig. 7). The baryonic mass is too small a part of the total mass to matter much to the problem, even within the optical edge of LSB disks. Evolutionary regulation simply can *not* solve the problem.

## 5.3. Formation

The evolutionary parameters just discussed fail to have an impact on the problem because LSB galaxies are dark matter dominated throughout. The evolution of the baryonic disk is almost irrelevant. This leaves the conditions of formation.

### 5.3.1. Variations in the Baryon Fraction

To explain the  $\Upsilon_o$ - $\Sigma_0$  relation using the baryon fraction  $f_b$ , one can simply assume that halos contain different amounts of baryons. This is of course just an ad-hoc assumption. Nominally, one would expect a universal baryon fraction with some modest amount of cosmic scatter.

This approach requires that the baryon fraction be uniquely related to the disk central surface

brightness:

$$f_b \propto \Sigma_0^{1/2}. \quad (15)$$

Since the Tully-Fisher relation must be maintained with  $\mathcal{M} \propto L \propto \Sigma_0 h^2$ , equation (15) implies  $\mathcal{M} \propto h^2 f_b^2$ . Halos of a given  $\mathcal{M}$  may have different baryon fractions, but somehow form larger or smaller disks to counterbalance this. Halos with low  $f_b$  must make up the deficiency in luminosity they suffer from low surface brightness by forming larger disks:  $f_b \propto h^{-1}$ . Why this should be the case is unclear. Beyond stating these requirements, little can be said because the hypothesized solution is so arbitrary.

### 5.3.2. Enclosed Mass and Spin

The situation is only a little better with  $\lambda$ . In this case, the requirement is

$$\lambda \propto \Sigma_0^{-1/2}. \quad (16)$$

Since  $\lambda = \mathcal{M}(R_o)/\mathcal{M}_T \approx R_o/R_H$ , the difference in this case is that the disks of lower surface brightness galaxies stretch further out into their halos. This has the built-in virtue of explaining the increasing dark matter domination of lower surface brightness disks while keeping the global baryon fraction fixed. In effect, this asserts that the mass density  $\sigma(R)$  is unrelated to the surface brightness  $\Sigma(R)$ . Then, if  $\sigma$  is a constant in equation (8), the lack of a shift in the Tully-Fisher relation follows and the  $\Upsilon_o$ - $\Sigma$  relation just reflects the difference in  $\sigma(R)$  and  $\Sigma(R)$ . We measure increasing mass to light ratios with decreasing surface brightness because  $\Upsilon_o(R_o)$  just measures a systematically greater portion of the global  $\Upsilon_T$ :  $\Upsilon_o/\Upsilon_T \sim R_o/R_H \sim \lambda \sim \Sigma_0^{-1/2}$ .

A consequence of this approach is that measuring one parameter of the optical light distribution, the central surface brightness, immediately tells one the extent of the dark matter relative to the light. Specifying the distribution of either  $\lambda$  or  $\Sigma$  immediately determines the distribution of the other. By the variational principle,

$$\frac{\delta \Sigma}{\Sigma} = -2 \frac{\delta \lambda}{\lambda}. \quad (17)$$

Our parameter  $\lambda$  can be related to the theoretical concept of the spin parameter

$$\lambda_s = \frac{\mathcal{J}|E|^{1/2}}{G\mathcal{M}^{5/2}} \quad (18)$$

(Peebles 1971). This parameterizes the angular momentum acquired by protogalaxies from tidal torques. The details of this process are uncertain, but all that matters here is that *within this framework* dissipative baryonic collapse is halted by angular momentum. Collapse from the initial  $\lambda_s$  of the halo and protogalaxy stops when  $\lambda_s^{disk} \rightarrow 1$ . This gives the condition  $\lambda \approx R_o/R_H \approx \lambda_s$ . Objects with high primordial spin  $\lambda_s$  will collapse less than low spin objects.

Presuming that spin is the underlying reason for  $\lambda$  provides a test. Equations (18) and (19) give the mapping from spin to surface brightness:

$$\mu_0 = 5 \log \left( \frac{\lambda_s}{\lambda_s^*} \right) + \mu_0^*. \quad (19)$$

This can be used to compare the observed distribution  $\phi(\mu_0)$  (McGaugh 1996a; de Jong 1996b) with the spin distribution predicted by numerical models. We are free to fit the parameters  $\lambda_s^*$  and  $\mu_0^*$  in order to obtain a fit, but the shapes of the distributions are specified by equation (19) and hence provide a test.

There have been various theoretical attempts to predict the distribution of the spin parameter (e.g., Efstathiou & Jones 1979; Barnes & Efstathiou 1987; Eisenstein & Loeb 1995; Steinmetz & Bartelmann 1995). These are all rather uncertain. Nevertheless, there seems to be general consensus that the distribution of spins is broad and approximately symmetric about some typical value,  $\lambda_s \approx 0.07 \pm 0.03$ . Two typical examples are plotted together with the surface brightness data in Fig. 8 for  $\lambda_s^* = 0.03$  and  $\mu_0^* = 21.5$ . These values are chosen to put the theoretical distributions in the same vicinity as the data, but we do not attempt a formal fit because of the great uncertainty in the predicted spin distribution. A tolerable match is found given the large error bars.

At the moment, there is no test in the shape of the surface brightness distribution at the low surface brightnesses. Because of the stretching imposed by equation (19), the theoretical prediction of the spin distribution needs to be made at quite high resolution in  $\lambda_s$  to provide a useful test. Similarly, the observed surface brightness distribution needs to be determined to much greater accuracy.

A sharp feature in the surface brightness distribution occurs at high surface brightness which is not reflected in the spin distributions. The  $\lambda_s \rightarrow \mu_0$  picture predicts a large number of high surface brightness disks which are not found observationally. In order to match the high surface brightness cut off, one must invoke some critical phenomenon at  $\lambda_s^* \approx 0.03$ . For example, one might suppose that protogalaxies with  $\lambda_s < 0.03$  fail to form disks, perhaps becoming ellipticals instead. This might plausibly come about if destructive disk instabilities set in when a critical surface density is exceeded.

The environmental dependence of  $\mu_0$  and  $\lambda_s$  provides a constraint which is independent of  $\phi(\mu_0)$ . The numerical simulations generally agree that  $\lambda_s$  is only weakly correlated with environment (Steinmetz & Bartelmann 1995) if at all (Barnes & Efstathiou 1987). In contrast, putatively high spin LSB galaxies very clearly reside in low density environments (Schombert et al. 1992; Bothun et al. 1993; Mo et al. 1994). It is thus difficult to understand the observed environments of LSB galaxies if spin is the principal parameter determining the surface brightness.

## 6. Rotation Curve Shapes

So far, we have only discussed possible interpretations of observational fact (1), the universality of the Tully-Fisher relation. That is, we have only attempted to understand why  $V_c$  is correlated with  $L$ . This proves difficult since  $L \propto V_c^4$  does not follow from  $V^2 = GM/R$ . The full shapes of the rotation curves complicate matters even further.

### 6.1. Expectation Values

In order to interpret the shapes of rotation curves, it is necessary to establish some prior expectation. This requires a deeper investigation of the subject of galaxy formation than we have made so far. Galaxy formation is a difficult subject, and even very sophisticated modeling efforts have yet to reach the point where the formation and evolution of an individual galaxy can be studied in detail. Building sophisticated models requires specifying a cosmology and deciding what the dark matter is. Our interest here is in placing constraints free of such assumptions, so we take a different tack. We construct two models which illustrate the most obvious possibilities. We intentionally keep these models simple to illustrate the important physical ideas. More complex models are usually special cases of one or the other.

Disk galaxies are thought to be composed of two basic components: a dynamically cold disk and a dynamically hot dark matter halo. To construct our models, we will assume that the disk is purely exponential. This is not precisely true of course, but it is an adequate approximation for our purposes. We will also make the usual assumption that dark matter halos are isothermal spheres.

The density distribution of the dark matter is taken to be

$$\rho(R) = \frac{\rho_C}{1 + (R/R_C)^2} \quad (20)$$

where  $\rho_C$  is the core density and  $R_C$  is the core radius. This density distribution is divergent with an infinite total mass, so there must be an additional parameter  $R_H$  to describe the outer edge of the halo. The effects of  $R_H$  are not apparent in the collected data. Experimenting with the models indicates that effects due to  $R_H$  would be apparent if observations were anywhere near reaching it, so it can be ignored for now. The rotation curve resulting from this mass distribution is

$$V_{halo}(R) = V_H \sqrt{1 - \frac{R_C}{R} \tan^{-1} \left( \frac{R}{R_C} \right)} \quad (21)$$

where the asymptotic circular velocity is  $V_H = \sqrt{4\pi G \rho_C R_C^2}$ . This gives rise to asymptotically flat rotation curves with  $V_c \rightarrow V_H$  as  $R \rightarrow \infty$ . Note, however, that the flatness of observed rotation curves at finite  $R$  depends on a delicate balance between disk and halo components (the disk-halo “conspiracy”).



The rotation curve of a thin exponential disk (Freeman 1970) is

$$V_{disk}(R) = \sqrt{4\pi G\sigma_0 h y^2 [I_0(y)K_0(y) - I_1(y)K_1(y)]} \quad (22)$$

where  $y = R/2h$ ,  $\sigma_0$  is the mass surface density corresponding to the central surface brightness, and  $I_n$  and  $K_n$  are modified Bessel functions of the first and second kind.

### 6.1.1. *Simple, General Model Galaxies*

We construct toy galaxy models based on these mass distributions and two simple ideas. One hypothesis is that LSB galaxies are diffuse because their dark matter halos are diffuse. We will refer to this hypothesis as “density begets density,” or DD for short. In DD, differences in surface brightness are driven by the differences in the amplitude of the original density fluctuations  $\delta$  from which galaxies arise. The other hypothesis is that galaxies of the same mass live in the same halos, but that the relative extent of the disk varies. This is essentially the same as the  $\lambda$ - $\Sigma$  relation discussed above, and we will refer to this as the “same halo” hypothesis, or SH for short. In SH, differences in surface brightness are driven by differences in the spin parameter  $\lambda$ .

In both cases, there is a spectrum of masses which are the main factor determining the total luminosity. The surface brightness is principally determined by  $\delta$  and  $\lambda$  in DD and SH respectively. This is not to say that mass maps directly to luminosity and  $\delta$  or  $\lambda$  directly to surface brightness, merely that these are the strongest relations. In principle, there are theoretical distribution functions  $\Phi(\mathcal{M}, \delta)$  (e.g., Mo et al. 1994) and  $\Phi(\mathcal{M}, \lambda)$  (e.g., Dalcanton et al. 1997) which somehow transform to the observable bivariate distribution  $\Phi(M, \mu_0)$ . The transformation need not be free of axial twists; in both cases one expects some weak correlation between luminosity and surface brightness. A complete theory should convolve the distributions of  $\mathcal{M}$ ,  $\delta$ , and  $\lambda$  and incorporate the physics of star formation to obtain luminosity and surface brightness from the calculated baryonic mass distribution. This is beyond current abilities. However, we are concerned here merely with establishing a basic expectation for the dependence of  $V(R)$  on surface brightness. For this simple purpose, it suffices to fix the principal luminosity determinant (mass) and look at the effects of variation in density and spin.

**Density begets Density:** The DD hypothesis is motivated by a number of observations (McGaugh 1992, 1996b). Principle among these is that the observed surface density of gas and stars is low in LSB galaxies. This will occur naturally if LSB galaxies arise from low density peaks in the initial fluctuation spectrum. At a given mass, small  $\delta$  peaks will turn around and collapse at a later time. They should also have a larger virialization radius and hence have a lower density of dark as well as luminous matter. A collapse time which is somewhat later for LSB than HSB galaxies is suggested by the ages inferred from their colors (McGaugh & Bothun 1994; Rönnback & Bergvall 1994; de Blok et al. 1995). That LSB galaxies should be associated with low

( $\sim 1\sigma$ ) density peaks is often asserted as obvious, and is indeed well motivated by all the physical properties of LSB galaxies (colors, metallicities, and gas contents) as well as actual densities (de Blok & McGaugh 1997). The DD hypothesis makes three important predictions which have subsequently been tested. One is that LSB galaxies should be less strongly clustered than HSB galaxies. There should be a shift in the amplitude of the correlation function  $\xi(r)$  by an amount corresponding to the difference in the amplitudes of the perturbations  $\delta$  from which the galaxies arose. This was confirmed by Mo et al. (1994). The second prediction is that LSB galaxies should have slowly rising rotation curves, in qualitative agreement with the data. The third prediction is that LSB galaxies should *not* fall on the same Tully-Fisher relation as HSB galaxies, in flat contradiction to the observations.

**Same Halo:** The SH hypothesis is motivated by the Tully-Fisher relation. It presumes that  $V_c$  is determined by  $V_H$ ; the halos are identical regardless of surface brightness so a single Tully-Fisher relation is assured. LSB disks are more dark matter dominated than HSB disks simply because they extend further out into their halos. Aside from the Tully-Fisher relation, SH enjoys none of the observational successes which motivated the DD model. There should be no age difference: all halos of the same mass collapse at the same time. This is not a strong objection, as it is difficult to distinguish age from a slow evolutionary rate (e.g., McGaugh & de BlokMdB 1997). A more serious problem with SH is that it does not predict the observed shift in the correlation function: spin and environment are not correlated (Steinmetz & Bartelmann 1995; Barnes & Efstathiou 1987). An additional environmental effect must be invoked to produce this. Whatever mechanism causes LSB galaxies to be isolated must be quite strong, as their isolation is clear out to  $> 1$  Mpc (Bothun et al. 1993). This is much too large a range for tidal forces to be effective, especially as the dark matter domination of LSB galaxies makes them quite robust against even strong tidal encounters (Mihos et al. 1997). Yet so compelling is the constraint imposed by the Tully-Fisher relation that a number of models for the formation of LSB galaxies have already appeared which are primarily motivated by this observation (e.g., Dalcanton et al. 1997; Navarro 1996a). Though more complicated than our illustrative SH model, these models reduce to the same basic scenario, and enjoy the same virtues and suffer the same vices as SH.

The level  $V_c$  of the flat part of the rotation curve is only one piece of the information contained in  $V(R)$ . The full shape of the rotation curves provide the most complete test of both DD and SH hypotheses. To see what these predict, let us construct a nominal HSB model with  $h = R_C = 1$  (Fig. 9). In general this is approximately true in HSB galaxies (e.g., Athanassoula et al. 1987; Broeils 1992; Rhee 1996; de Blok & McGaugh 1997) which are frequently modeled in this way (e.g., Hernquist 1993). We assume the disks are maximal with  $V_{disk}^{peak} \approx V_H$ , as suggested by the disk-halo conspiracy. This is a conservative assumption for testing the shapes of rotation curves, since the differences between HSB and LSB halos are minimized in this case (de Blok & McGaugh 1997). In practice, this means  $V_H = \sqrt{\pi G \sigma_0 h} = 1$ . This results in  $V_{disk}^{peak} \approx 0.8 V_{total}(2.2h)$  as found empirically in HSB galaxies (de Blok & McGaugh 1997).

The resulting null HSB model is plotted in the top panels of Fig 9. The expected shape of the rotation curve of an LSB galaxy (bottom panels of Fig 9) follows from the null HSB model and each hypothesis by simple scaling. We assume that the mass of the HSB and LSB galaxy are the same, both disk and halo, so that the baryon fraction is the same. The same disk mass imposes the requirement that  $\sigma_0 h^2$  be the same. This gives the scaling required to calculate the rotation curves under each hypothesis. For illustration, we choose  $h(\text{LSB}) = 3$  (the difference between NGC 2403 and UGC 128) which gives  $\sigma_0(\text{HSB})/\sigma_0(\text{LSB}) = 9$  to conserve mass.

Under the DD hypothesis, the halo should be diffuse like the disk. We assume  $R_C = h(\text{LSB}) = 3$ . This is not the only possibility, but all that matters for this test is that there is some stretching of the halo. The resulting rotation curve is plotted in the lower left panel of Fig. 9. This is essentially just a stretched version of the HSB model, sharing the same disk-halo conspiracy but not the same  $V_c$  since  $R$  is larger in  $V^2 = GM/R$ .

Under the SH hypothesis, the halo is the same so  $R_C = 1$  even though  $h(\text{LSB}) = 3$ . For the baryon fractions to be the same, the LSB galaxy must reach to much nearer the edge of the halo than the HSB, though this is presumably still a long way off. The resulting  $V(R)$  is dominated by the halo at all radii, and by construction reaches the same  $V_c$ .

We can now test the models against the data. The HSB model has been constructed to typify a disk with the Freeman central surface brightness  $\mu_0 = 21.65$ . The LSB model is a factor of 9 lower in surface density, corresponding to  $\mu_0 = 24.04$  assuming  $\Upsilon_*$  is similar. There are four galaxies with reasonable data within 0.2 mag of this surface brightness. These are plotted in Fig. 10 by scaling  $R$  by the observed scale length  $h$  and  $V$  so that  $V_c = 1$ .

The data are not well predicted by either model. The DD model predicts a gradual rise of  $V(R)$  which is indeed seen at small  $R$ . However,  $V(R)$  continues to rise to a level  $V_c$  well in excess of that anticipated by DD, which does not predict a universal Tully-Fisher relation. The SH model has the correct  $V_c$  (indeed, it was constructed to do just this), but predicts that  $V(R)$  should rise much more rapidly than it actually does. To be consistent with observations, the halos of LSB galaxies must indeed be more diffuse (the basis of the DD model). Yet somehow they must also attain the  $V_c$  dictated by the Tully-Fisher relation (the basis of SH).

Neither DD nor SH alone adequately explain the observations. It seems that some hybrid is required. Perhaps a convolution of the  $\delta$  and  $\lambda$  distributions is needed, with both initial density and spin contributing to determine the surface brightness. Indeed, a proper theory should account for both effects; these simple models assume one or the other dominates.

The hybrid approach has its own problems. To match the environments of LSB galaxies and the slow rate of rise of their rotation curves, DD must make a substantial contribution to the hybrid. However, any mixing of DD with SH degrades the latter's ability to explain the Tully-Fisher relation. A perceptible shift in the normalization with surface brightness would be introduced, and the scatter would increase.

Having argued that neither model nor a hybrid is adequate, we note that the DD model was able to explain many of the observations of LSB galaxy densities and ages, and did successfully predict the slow rate of rise of LSB galaxy rotation curves and the shift in the correlation function (Table 3). Yet it is made very implausible by LSB galaxies obeying the Tully-Fisher relation. Why a model should be successful in many respects and yet fail on one important point is a puzzle. But fail it does, so in the following section we examine more elaborate models to see if they fare any better.

### 6.1.2. *Complex, Specific Model Galaxies*

Until now, we have intentionally kept our models simple so that genuine predictions can be identified and tested. More complex models necessarily have more parameters and generally assume a specific cosmogony. Many make no specific predictions which are actually testable. However, some do, and we examine these here.

A more elaborate version of the SH model is given by Dalcanton et al. (1997). They give a detailed model which specifically incorporates LSB galaxies and makes testable predictions about them. In essence this is an elaboration of SH and shares the same virtues and vices. As such, it does have the correct Tully-Fisher relation, with LSB disks reaching further out into the halo than HSB disks. Consistency with the Tully-Fisher relation is not a prediction, it is a construction motivated by the data. The initial prediction of the same physical scenario does predict a shift in the Tully-Fisher relation for LSB galaxies (Dalcanton et al. 1995).

Nevertheless, the model of Dalcanton et al. (1997) does have the virtue of making a number of specific, bona-fide predictions about the bivariate distribution  $\Phi(\mu_0, h)$  (their Fig. 2), the differential luminosity density as a function of surface brightness  $J(\mu_0)$  (their Fig. 7), and the shapes of the rotation curves (their Figs. 1 and 8). At this time, the bivariate distribution is too ill-determined observationally to provide a good test. The best available estimate of  $\Phi(\mu_0, h)$  is provided by de Jong (1996). It has sharp features which are not obviously consistent with the smooth prediction of  $\Phi(\mu_0, h)$ , but the error bars are sufficiently large that it is not obviously inconsistent except for very high surface brightnesses. Here, many more galaxies are predicted than observed. This is the same problem already discussed for  $\lambda$ - $\Sigma$  in §5.2 and Fig. 8.

The differential luminosity distribution  $J(\mu_0)$ , though still rather uncertain observationally, currently provides a test which is less sensitive to assumptions about the size distribution. The predictions of Dalcanton et al. (1997) are reproduced together with the available data (as per McGaugh 1996a) in Fig. 11. The model overpredicts the luminosity density in HSB galaxies just as it overpredicts their number. It also overpredicts the luminosity density due to LSB galaxies. The predicted distribution is broad and continuous unlike the sharp featured  $J(\mu_0)$  which is observed. However, the disagreement at the faint end is not terribly severe, so the model might be salvaged by imposing a cut off at the bright end. Disk stability might provide such a mechanism, since at

some high surface density, disk self gravity will become so dominant that the usual instabilities set in.

A stronger test is provided by the shape of the rotation curves. The model makes specific choices for the baryon fraction and mass to light ratio which need not be precisely correct. To circumvent this and obtain a test which is independent of these assumptions, we use the information provided by Fig. 1 of Dalcanton et al. (1997) to construct directly observable quantities. For each model of a given mass and spin ( $\mathcal{M}, \lambda_s$ ), we extract the disk scale length  $h$  and the radius  $R_{34}$  where  $V(R_{34}) = 3/4 V_c$ . These can be combined to give a dimensionless ratio  $R_{34}/h$  which measures the rate of rise of the rotation curve independent of most model assumptions and directly is relatable to observations.

The choice of  $R_{34}/h$  is motivated by Fig. 9, which shows that the rate of rise of the inner portion of  $V(R)$  provides the most sensitive test of SH models. We choose  $3/4$  of  $V_c$  rather than  $1/2$  because resolution can affect the estimate of  $V$  at small  $R$ . For this test we only use galaxies resolved with at least 8 beams across the diameter corresponding to  $R_{34}$ . Note that this test is independent of inclination, so we can use galaxies from Table 2 which are adequately resolved and for which  $V_c$  is well defined.

The data and model predictions are plotted in Fig. 12. The rate of rise of  $V(R/h)$  is clearly correlated with both luminosity and surface brightness in the sense that brighter galaxies have more rapidly rising rotation curves. The correlation with absolute magnitude is particularly clear, consistent with other work (Persic et al. 1996). This is not to say that we confirm the precise functional form Persic et al. (1996) suggest for the “universal rotation curve,” but it is true that to first order luminosity is a good predictor of the shape of  $V(R/h)$ . As with the Tully-Fisher relation, the same result applies to both HSB and LSB galaxies, and is not a selection effect stemming from samples limited only to one or the other.

Also shown in Fig. 12 are curves constructed from the models of Dalcanton et al. (1997). These can be shifted or stretched in the abscissa by changing the assumed  $\Upsilon_*$  or inserting a  $\mathcal{M}$ - $\lambda_s$  correlation. Curves are shown for  $\mathcal{M}$  independent of  $\lambda_s$  and for a relation which on average gives  $L \propto \Sigma^{1/3}$  as Dalcanton et al. (1997) predict. The model parameters have been well chosen to reproduce the observed range of  $M_B$  and  $\mu_0$ . However, they are far too low in  $R_{34}/h$ :  $V(R)$  is predicted to rise much more rapidly than observed, just as in the simple SH model.

Though it is possible to shift the models along the abscissa, the same is not true for the ordinate. The nearly order of magnitude offset in  $R_{34}/h$  is a serious problem. Worse, the predicted run of  $R_{34}/h$  with  $M_B$  is orthogonal to the observations in Fig. 12(a). This can not be cured by a simple offset. The shape of the model curve is also wrong in Fig. 12(b), with  $R_{34}/h$  decreasing slightly over most of the range of  $\lambda_s$  where in fact it should continue to increase. Hence, the inner shape of the observed rotation curves is a serious problem for the Dalcanton et al. (1997) model.

The severe normalization problem encountered by this  $\lambda_s$  driven model could be helped by using isothermal halos rather than Hernquist or Navarro profiles as has been done. However, this

provides an additional parameter, the core radius. It is  $R_C$  which controls the shape of rotation curves (equation 21), so it will always be possible to obtain an adequate solution by making  $R_C$  an appropriate function of  $M_B$ . The challenge then is to understand why halos have finite core radii contrary to the expectations of many numerical simulations (Dubinski & Carlberg 1991; Navarro et al. 1996; Cole & Lacey 1996), and additionally why  $R_C$  assumes the particular value required at each  $M_B$  (Casertano & van Gorkom 1991).

Flores et al. (1993) describe a  $\lambda_s$  model which employs isothermal halos. They predict how the outer slope of rotation curves should depend on  $\lambda_s$  (their Figs. 5 and 6c) which should lead to a segregation of the data by surface brightness in these plots. This is not apparent in our data, but the predicted amplitude of the effect is too small relative to the uncertainties for this to provide a useful test. We can note that, by their own stipulation, the model of Flores et al. (1993) is only viable for a fairly narrow range of parameters:  $f_b \approx \langle \lambda_s \rangle \approx 0.05$  and  $R_c/R_{tr} > 0.2$ . The truncation radius  $R_{tr}$  is the radius beyond which no baryonic infall occurs. The low required baryon fraction is not consistent with that determined from clusters of galaxies (e.g., Evrard et al. 1996); they can not both be correct. In the context of LSB galaxies the required truncation radius  $R_{tr}$  seems to be too small. Flores et al. (1993) state that the cooling time places an upper limit on the truncation radius so that

$$R_{tr} < 100 \left( \frac{f_b}{0.1} \right)^{1/2} \left( \frac{V_c}{300 \text{ kms}^{-1}} \right)^{1/2} \left( \frac{H_0}{100 \text{ kms}^{-1} \text{ Mpc}^{-1}} \right)^{-1/2} \text{ kpc.} \quad (23)$$

For a galaxy like Malin 1, this gives  $R_{tr} \approx 58$  kpc which is only one disk scale length (Bothun et al. 1987). The disk extends much further than this, and the baryons should have originated at even larger radii in this sort of collapse model. Though Malin 1 is an extreme example and equation (23) is subject to modification, the problem is generic to LSB galaxies. Upper limits on their baryon fractions (§7.2; de Blok & McGaugh 1997) are comparable to the value  $f_b \approx 0.05$  preferred by Flores et al. (1993). This means either that the true  $f_b$  is much lower than tolerable, or that LSB galaxies have collapsed so little that they sample the initial baryon fraction:  $R_o \approx R_{tr}$ . This implies very high spin,  $\lambda_s \sim 1$ . The highest spin considered in any model is around  $\lambda_s \sim 0.2$ .

Since sophisticated models are unable to explain any more than the simple DD and SH models, one wonders if perhaps the answer lies in the complex interplay between dark matter, gas hydrodynamics, and star formation during galaxy formation. A fundamental assumption of  $\lambda_s$  models is that angular momentum is conserved and not transferred between dark and luminous components. Numerical models indicate that angular momentum transfer does indeed occur (Katz & Gunn 1991).

There has been a great deal of progress on numerical models which incorporate hydrodynamics. One promising example which makes testable predictions for galaxies is that of Cen & Ostriker (1993). Their Fig. 3 predicts the trend of total mass and cold gas mass with stellar mass, and is reproduced here in Fig. 13 together with the data.

The data are plotted in Fig. 13(a) assuming  $\Upsilon_* = 2$  and for a dynamical mass within a radius

of  $R = 5h$ . The precise value assumed for  $\Upsilon_*$  makes no difference on this logarithmic plot which spans many decades. A different choice for  $R$  simply translates the dynamical mass vertically. The trend predicted by Cen & Ostriker (1993) qualitatively mimics that of Fig. 4(a). However, they predict a much stronger change of  $\mathcal{M}_T$  with  $\mathcal{M}_*$  than is actually observed. The difference between the slope of the data and that of the line of constant  $f_b$  is barely perceptible.

Presumably, halos extend further than  $R = 5h$ . Some of the data could be shifted into agreement with the models by an appropriate choice of  $R$ , but not all of it at once. This could only be done by forcing  $R_H$  to be an appropriate function of  $\mathcal{M}_*$ , i.e., by inserting the answer. Unfortunately, there is no test here. The simulations predict  $\mathcal{M}_T$  but not  $\mathcal{M}(R)$ , while observations can only probe the latter.

There is a test in the other panel of Fig. 3 of Cen & Ostriker (1993). This is a prediction of the cold gas mass as a function of stellar mass, and is reproduced in Fig. 13(b). This is an important test of any hydrodynamical model which attempts to model the gas physics of galaxy formation. Data for spiral galaxies are taken from McGaugh & de Blok (1997), and that for elliptical galaxies from Wiklind et al. (1995) with  $\Upsilon_*$  computed following the relation of van der Marel (1991). The model prediction is orthogonal to the data, and off by five orders of magnitude at the bright end.

It would appear that numerical models are as yet a long way from producing realistic galaxies (see also Navarro & Steinmetz 1997).

## 6.2. More Fine Tuning Conspiracies

The fundamental problem is this: one needs pieces of both the DD and SH models, yet grafting them together always results in a serious fine-tuning conspiracy. Recall that  $V_H \propto \sqrt{\rho_C} R_C$ . To satisfy the Tully-Fisher relation (Fact 1),  $V_c$ , and hence the product  $\rho_C R_C^2$ , must be the same for all galaxies of the same luminosity. Lower surface brightness galaxies have rotation curves which rise more gradually than those of higher surface brightness galaxies of the same luminosity (Fact 2). To decrease the rate of rise of the rotation curves as surface brightness decreases,  $R_C$  must increase (equation 21). Together, these two require a fine-tuning conspiracy to keep the product  $\rho_C R_C^2$  constant at fixed luminosity while  $R_C$  must vary with the surface brightness. That is,  $V_H \propto \sqrt{\rho_C} R_C$  stays fixed while  $R_C$  and  $\sqrt{\rho_C}$  oscillate up and down as dictated by  $\mu_0$ . The  $\Sigma_0$ - $\Upsilon_0$  conspiracy has grown into one tying the optical and halo parameters intimately together.

Though both DD and SH and their variants do not work, there is a very clear need to keep  $V_H$  fixed (as in SH) and an equally clear need to vary  $R_C$  (as in DD). The exact amount of variation depends on how the disk-halo decomposition is treated (de Blok & McGaugh 1997). For example, in the maximum disk case, much of the variation in  $R_C$  is transferred to  $\Upsilon_*$ , resulting in a systematic increase of  $\Upsilon_*$  as  $\Sigma_0$  decreases, opposite the sense indicated by the colors. The problem simply shifts from one parameter to another. In general, introducing more parameters

just increases the number of things which must be fine tuned.

To be successful, structure formation models must reproduce this peculiar behavior.

## 7. Flavors of Dark Matter

In this section, we examine constraints that our data can place on the various hypothesized forms of dark matter. Ideally, this requires testable predictions for each. There are some, but not many. The issue of dark matter has always been data driven. As a result, the process is often more a matter of examining the sensibility of previous data-based inferences with the expanded dynamic range of the present data.

### 7.1. Cold Dark Matter

Perhaps the leading candidate for the dark matter is CDM. This DM candidate is composed of dynamically cold massive particles. Usually imagined to be some hypothetical fundamental particle (e.g., WIMPs or Axions), CDM could also be massive black holes or some other entity which only interacts gravitationally. Here we are concerned with only the dynamical effects, since this is all that defines CDM. By stipulation, there is very little else about it that can be tested. This is both a virtue and a vice, since DM candidates which are relatively easy to detect (e.g., faint stars) are more easily falsified.

Nevertheless, CDM has many genuine virtues. A non-baryonic form of dark matter is required to reconcile dynamical measures of the cosmic density ( $\Omega \gtrsim 0.2$ ; e.g., Davis et al. 1996) with the low density of baryons indicated by primordial nucleosynthesis ( $\Omega_b \lesssim 0.03$ ; Fields et al. 1996; Copi et al. 1995). An important aspect of CDM is that it does not respond to radiation pressure. It can therefore begin to clump and form structure early without leaving too much of an imprint on the microwave background. Indeed, this was another motivation for inventing CDM, since it is not otherwise possible to get from the very smooth universe that existed at the time of recombination to the very clumpy one we see today.

These two facts,  $\Omega \gg \Omega_b$  and the lack of structural imprint on the microwave background demand CDM. Indeed, the ability of CDM models to hide anisotropies in the microwave background far below the upper limits of various experiments was considered a great success until fluctuations were actually measured by COBE (Bennett et al. 1994). These are at a level much higher than expected in standard  $\Omega = 1$  CDM.

The shape of the power spectrum  $P(k)$  predicted by standard CDM has been clearly falsified (e.g., Fisher et al. 1993). The expectation  $P(k) \propto k^n$  with  $n = 1$  is not so much a bona-fide prediction as the physically most plausible case. So it is possible to repair CDM after the fact. Ideas for doing this include “tilting” the spectrum (twiddling  $n$ ), lowering  $\Omega_{CDM}$ , adding an



admixture of hot dark matter to boost  $P(k)$  on large scales, or invoking the cosmological constant. Indeed, it appears necessary to do several of these things (Ostriker & Steinhardt 1995).

Even so, there are no dark matter candidates more viable than CDM, which does at least make some testable predictions. For example, the mass function of galaxies is directly calculable, and can be used to predict the observed luminosity function. It is very difficult to reconcile the two (Heyl et al. 1995). One expects a much higher ( $> 300 \text{ kms}^{-1}$ ) pairwise velocity dispersion than is observed ( $< 100 \text{ kms}^{-1}$ ; Cen & Ostriker 1993; Governato et al. 1997). Though structure forms rapidly in CDM, CDM scenarios have considerable difficulty in explaining the presence of large disks (Prochaska & Wolfe 1997) and hot clusters (Donahue et al. 1997) at high redshift. It also anticipates (Kaiser 1986) rapid evolution in the cluster X-ray luminosity function which is not observed (Scharf et al. 1997; Burke et al. 1997; Rosati et al. 1997).

Another important test is whether LSB galaxies are biased relative to HSB galaxies. This clearly is not as strong an effect as would be required if  $\Omega = 1$  (Pildis et al. 1997), but does occur in the expected sense (Mo et al. 1994). This is a definite success, but not one specific to CDM. The tendency for low density galaxies to reside in low density regions is a generic consequence of bottom-up structure formation.

A very important, testable, bona-fide prediction of CDM has recently been made by Navarro et al. (1996) and Cole & Lacey (1996); see also Dubinski & Carlberg (1991). They show that individual CDM halos have a universal structure profile. These take the form

$$\rho_{CDM}(R) = \frac{\rho_i}{(R/R_s)(1 + R/R_s)^2} \quad (24)$$

where  $R_s$  is the characteristic radius of the halo and  $\rho_i$  is related to the density of the universe at the time of collapse. These parameters are not independent and are set by the cosmology. The concentration of the resultant halo is encapsulated in the concentration parameter  $c = R_{200}/R_s$ .  $R_{200}$  is the radius where the density contrast exceeds 200, roughly the virial radius. This establishes a clear expectation value for the mass distribution and resultant rotation curves of CDM halos, which are

$$V(R) = V_{200} \left[ \frac{\ln(1 + cx) - cx/(1 + cx)}{x[\ln(1 + c) - c/(1 + c)]} \right]^{1/2}, \quad (25)$$

where  $x = R/R_{200}$  (Navarro et al. 1996). The velocity  $V_{200}$  is characteristic of the halo, and is defined in the same way as  $R_{200}$ . The halo rotation curve is thus specified by two parameters,  $V_{200}$  and  $c$ , which give the total halo mass and the degree of concentration of that mass.

Low surface brightness galaxies are a good place to test this prediction as their disks are dynamically insignificant: the rotation curves provide a direct map of the dark mass distribution. The strongest test is afforded by the lowest surface brightness galaxy with the best resolved rotation curve. Surface brightness is important because it is related to the rate of rise of the rotation curve which constrains the concentration parameter. Resolution is important because we

wish to test the shape of the rotation curve specified by equation (25). The galaxy which best suits these requirements is F583–1.

In order to compare observations with theory, we need to do several things. Observationally, we wish to remove the influence of the known baryonic component and isolate the dark matter. This is done by assuming the maximum disk mass of de Blok & McGaugh (1997). Both full and corrected rotation curves are shown in Fig. 14, where it can be seen that the assumption about the optical disk mass is irrelevant. This is the virtue of using LSB galaxies for this sort of test.

Theoretically, we need to specify an appropriate  $c$  and  $V_{200}$ . The concentration parameter depends on the cosmology, for which we consider several possibilities using the halo characterization code provided by Navarro (1997, private communication). We will refer to three basic cases: standard CDM with  $\Omega = 1$  (SCDM), open CDM with  $\Omega = 0.3$  (OCDM), and a flat  $\Lambda$ -dominated cosmology with  $\Omega_\Lambda = 0.7$  ( $\Lambda$ CDM). Lower  $\Omega$  generally results in lower  $c$ , as does lower  $H_0$ . The latter is not a strong effect, so we retain a fixed  $H_0 = 75 \text{ kms}^{-1}\text{Mpc}^{-2}$ . Other parameters matter fairly little, except the normalization of the power spectrum which we fix to the COBE observations. Adopting another normalization, like that for rich clusters, has the fairly minor effect of interchanging the relative concentrations of the OCDM and  $\Lambda$ CDM cases: OCDM is the least concentrated model with a COBE normalization, but  $\Lambda$ CDM is the least concentrated for a lower normalization. This distinction is unimportant.

We shall see that the observations require extremely low  $c \lesssim 5$ . Such low concentrations are readily obtained only by lowering the power spectrum normalization to  $\sigma_8 < 0.2$ . This is completely inconsistent with either the COBE or the rich cluster normalization.

The last item we need is an estimate  $V_{200}$  or the mass of the halo, which is also a minor factor in determining  $c$ . This can be done in a variety of ways. Perhaps the most obvious is to use the observed baryonic disk mass as an indicator of the halo mass. The mass of the disk is reasonably well constrained by the maximum disk solution ( $\mathcal{M}_* \leq 4.5 \times 10^8 \mathcal{M}_\odot$ ) and the fact that most of the baryons are in directly observable atomic gas ( $\mathcal{M}_g = 2.4 \times 10^9 \mathcal{M}_\odot$ ). It is unlikely that any significant additional baryonic mass is in undetected forms (either molecular or ionized gas), and even factors of two here will not much affect the arguments which follow. The total baryonic mass of F583–1 is thus  $\mathcal{M}_{bar} \approx 2.9 \times 10^9 \mathcal{M}_\odot$ . This can be combined with a baryon fraction to give a halo mass. The universal baryon fraction is thought to be well measured by rich clusters of galaxies, giving  $f_b \approx 0.09$  (for  $H_0 = 75 \text{ kms}^{-1}\text{Mpc}^{-2}$ ; e.g., White & Fabian 1995). This then implies a halo mass of  $\mathcal{M}_H \approx 2.9 \times 10^{10} \mathcal{M}_\odot$ . Note that the maximum disk decomposition already implies  $\mathcal{M}_H \geq 2.2 \times 10^{10} \mathcal{M}_\odot$  (de Blok & McGaugh 1997), so either this disk is observed to very near the edge of its halo, or the baryon fraction determined in clusters is not universal (§8).

The concentration indices derived for these cases are listed in Table 4 and the results plotted in Fig. 14(a). The results are disastrous. The SCDM model grossly overpredicts the rate of rise of the rotation curve. The less concentrated OCDM and  $\Lambda$ CDM models do the same. Worse, all predict very much the wrong asymptotic velocity, as the halo mass appropriate for the observed

baryon mass gives  $V_{200} = 43 \text{ kms}^{-1}$  when  $V_c = 84 \text{ kms}^{-1}$ .

Part of the problem here is the well known failure of CDM models to simultaneously match the observed luminosity density and the normalization of the Tully-Fisher relation (e.g., Heyl et al. 1995; Frenk et al. 1996). Let us therefore try another approach. Navarro (1996a) suggests that the Tully-Fisher relation arises because  $V_c \approx V_{200}$  (though note that Navarro 1996b found that halo mass should not be well correlated with optical luminosity). By adopting  $V_{200} = 80 \text{ kms}^{-1}$ , we should at least come close to matching the outer portion of the rotation curve. This implies a much more massive halo,  $\mathcal{M}_H \approx 1.2 \times 10^{11} \mathcal{M}_\odot$ , and a correspondingly lower baryon fraction,  $f_b = 0.015$ .

This exercise again fails (Fig 14b). Only the lowest  $c$  model comes close to the observations, and even that predicts velocities which are too high for the dark matter. This is especially true in the inner parts, but remains true even in the outer parts where the normalization was set. Apparently, the Tully-Fisher relation does not arise from a simple equation of  $V_c$  with  $V_{200}$ . But if it does not, why does a Tully-Fisher relation with small scatter arise at all?

Note that the shapes of the observed rotation curves are not similar to the predicted shapes. Is it possible to fit the data with equation (25) at all? The answer would appear to be no. Fig. 14(c) gives several examples which come reasonably close by choosing  $c$  and  $V_{200}$  without regard to their cosmological origins. The model with  $c = 12$  gives a nicely flat rotation curve for the outer points, but grossly over predicts the inner rotation. Lower concentration models can be made to fit the interior points, but then get the exterior ones wrong. Equation (30) gives the wrong shape, and the clear prediction of CDM is simply not realized:

$$\rho_{CDM}(R) \neq \rho_{obs}(R). \quad (26)$$

Moreover, we do not have the freedom to fit  $c$  and  $V_{200}$  freely. The virtue of the model is that these are predicted once the cosmological parameters (especially  $\Omega$ ,  $P(k)$ , and  $f_b$ ) are stipulated. No plausible cosmology predicts  $(c, V_{200})$  which approximate the lowest surface brightness galaxies.

It has already been noted (Moore 1994; Flores & Primack 1994) that the steep interior density distribution ( $\rho_{CDM}(R) \propto R^{-1}$  at small  $R$ ) predicted by CDM is completely inconsistent with the few (4) analyzed observations of dwarf galaxies. These are all low surface brightness systems, which is the reason they are relevant. This problem of the shape of the rotation curves is general and clear in all of our data. We therefore confirm and extend the results of Moore (1994) and Flores & Primack (1994).

This situation admits three possibilities:

1. CDM is not the solution to the mass discrepancy problem;
2. CDM is correct but  $\rho_{CDM}(R)$  has not been correctly predicted; or
3. Both are correct but further physics intervenes to transform  $\rho_{CDM}(R)$  into  $\rho_{obs}(R)$ .

The second possibility seems unlikely. There is widespread agreement between independent modeling efforts (Dubinski 1994; Navarro et al. 1996; Cole & Lacey 1996). There is good physical reason for this agreement. Non-baryonic CDM only interacts gravitationally, with no way to set a preferred scale such as a core radius. This prediction of CDM seems very robust.

Within the framework of CDM, we are thus forced to consider the third possibility. This requires large scale mass redistribution which presumably results from the behavior of the baryonic component. The behavior of the baryons depends on such things as the hydrodynamics of gas flows and energy input from star formation, and is much more difficult to model than the CDM. Various possibilities for the effect of the baryons are generally referred to as “feedback” or sometimes as “gastrophysics.”

That feedback takes place at some level will modify the prediction that arises from CDM-only models. However, there is no guarantee that it will fix the problem under consideration. If we simply add feedback parameters to the model and tune them to match the observations, the model loses its predictive value.

There are three basic possibilities for mass redistribution:

1. Contraction of the CDM following dissipation of the baryons;
2. Orbital family redistribution at small radii; and
3. Expansion of the CDM following expulsion of baryons in galactic winds.

These might come about in a myriad of ways; we discuss the generic aspects of each in turn below. There is, however, a serious objection to any of them being important to large scale redistribution of the dark matter. In dark matter dominated LSB galaxies, baryons are a very small fraction of the total mass. To alter  $\rho(R)$  in the required fashion is a case of the tail wagging the dog.

The first possibility is that the dissipation of baryons during disk formation draws the dark matter distribution further in. This is sometimes called the adiabatic response of the halo to the disk, and should happen at some level (Dubinski 1994). It is relatively straightforward to model, but makes the problem *worse*. Halos which are initially too concentrated become even more so.

In order to model adiabatic contraction, one generally assumes that the baryons conserve angular momentum. This need not be the case, as numerical models indicate that a great deal of angular momentum can be transported to the dark matter (Katz & Gunn 1991). Such a process might result in the redistribution of orbital families, especially at small radii where the importance of the baryons is maximized. Such a redistribution might alter the cuspy nature of the initial CDM mass distribution. This process must transfer enough angular momentum to the dark matter to establish a large core radius, but not so much that it fails to form a rotationally supported baryonic disk. Simulations suggest that while some orbital redistribution does occur, it does not significantly impact  $\rho(R)$  (Merritt 1997).

The third possibility is the opposite of the first. Massive amounts of baryons are expelled. The dark matter follows gravitationally, thus establishing a more diffuse mass distribution. A frequently invoked mechanism for expelling the baryons is feedback due to violent star formation (e.g., Navarro et al. 1996c). There is one clear prediction of this scenario: galaxies explode and gas is lost. Yet the dim galaxies for which the need for mass redistribution is most severe are in fact very gas rich (McGaugh & de Blok 1997). In addition, a direct search for the residue of baryonic blow out resulted in non-detection (Bothun et al. 1992). It therefore seems unlikely that baryonic outflows can play a significant role in redistributing the dark matter.

Regardless of what mechanism is invoked, two drastic events are required to reconcile CDM with the observations. First, the baryon fraction must change by an order of magnitude from the universal value found in clusters. Second, the dark matter distribution must be radically changed from a Navarro et al. (1996) profile (equation 24) to something close to an isothermal sphere (equation 20). This is indeed a major transformation:  $\rho(R) \propto R^{-1} \rightarrow R^0$  at small  $R$  and  $\rho \propto R^{-3} \rightarrow R^{-2}$  at large  $R$ .

In many ways, CDM is superior to other hypothesized forms of dark matter. Most importantly, it does make some testable predictions. Unfortunately, these predictions persistently fail.

## 7.2. Hot Dark Matter

Another possible dark matter candidate is a massive neutrino. Though often invoked in the context of the solar neutrino problem, a massive neutrino does not help with the mass discrepancy problem in LSB galaxies. It has long been known that hot dark matter is good at forming structure on large scales (top-down), but not at making galaxies. In order for neutrinos to remain in dwarf galaxy halos, they would have to be much more massive than allowed by experiment (Lin & Faber 1983). It seems unlikely that mixing hot and cold dark matter would address the problems encountered by CDM alone, simply because the HDM component plays no role on the small scale of galaxies.

## 7.3. Baryonic Dark Matter

Baryonic dark matter is any form of hypothesized DM composed of ordinary matter. There are a great variety of hypothesized forms including brown dwarfs, very faint stars, Jupiters, and very cold molecular gas. The advantage of BDM is that baryons are known to exist. The problem is that BDM candidates are detectable, so most have been ruled out (Carr 1994).

The case in favor of BDM has been strengthened by the recent detection of microlensing events (e.g., Alcock et al. 1996). However, the detection of microlensing, a physical process which should at least occasionally occur, is not the same as the detection of BDM MACHOs. The clearest

result of these experiments is to rule out MACHOs as dark matter over many decades of mass, up to and including the most reasonable possibility of brown dwarfs (Ansari et al. 1996; Renault et al. 1997). Only if the lensing objects are surprisingly massive ( $\gtrsim 0.5M_{\odot}$ ) can MACHOs make up a significant fraction of the halo, and only then because this mass delimits the sensitivity range of the experiments. Sufficient statistics have yet to accrue to demand a significant halo mass fraction (Paczynski 1996), and there is no guarantee that the events observed to date are connected with the missing mass problem. Since particle physics analogies are often made for these experiments, we offer one of our own. The first thing one is likely to learn about is the background contaminants one did not expect (e.g., Zaritsky & Lin 1997).

A substantial amount of BDM suffers the two serious drawbacks which motivate CDM: the small amplitude of fluctuations in the microwave background and  $\Omega \gg \Omega_b$  from primordial nucleosynthesis. Although  $\Omega_b \gg \Omega_*$  is often invoked as an argument for baryonic dark matter, this can not explain the dynamical mass discrepancy or add up to the total  $\Omega$  (Dalcanton et al. 1994). To contemplate a conventional universe composed entirely of baryons, one must somehow dismiss both of these pillars of modern cosmology.

We are not aware of viable BDM scenarios which make specific predictions. Those which did have been ruled out. Nevertheless, there are several lines of argument favoring BDM. One is that light and dark matter are intimately coupled. This is certainly true (paper II). The potential for information transfer between the distinct dynamical components is maximized if they are cut from the same cloth. Another connection is that the ratio of atomic gas mass to dynamical mass  $\mathcal{M}_{HI}/\mathcal{M}_o$  seems to be roughly constant (Bosma 1981). This holds approximately true for LSB galaxies (see Fig. 13 of de Blok et al. 1996) as  $\mathcal{M}_{HI}/L$  and  $\Upsilon_o$  are both related to  $\mu_0$  with similar slopes.

A serious problem with this picture is the total failure of  $f_*$  to redress the  $\Upsilon_o$ - $\Sigma_0$  relation (Fig. 7). This occurs because a constant  $\mathcal{M}_{HI}/\mathcal{M}_o$  gives a constant shift in  $\log \Upsilon_o$ , not a systematic trend as required. The only way to salvage this picture would be to arbitrarily make the conversion factor  $\eta$  between  $\mathcal{M}_{HI}$  and total gas mass an appropriate function of  $\mu_0$ . That is, since  $\eta = 1.4$  strictly applies only to atomic gas, one might suppose that molecular gas becomes systematically more important with decreasing surface brightness. This would have to be an enormous effect to account for the large change in  $\Upsilon_o$ , and of course must be very systematic with surface brightness. This seems quite unreasonable, and in fact the opposite is observed: lower surface brightness galaxies appear to have substantially less molecular gas than higher surface brightness spirals (Schombert et al. 1990). An additional conspiracy must now be invoked: the  $CO/H_2$  conversion factor also varies systematically with surface brightness. This would have to be a big effect, but the size if not the systematic surface brightness dependence is already required if much of the dark matter is to be hidden in molecular form (Pfenniger et al. 1994).

Another motivation for BDM is that the outer shape of the rotation curve of HSB galaxies can sometimes be fit by scaling up the contribution of the HI. This suggests an additional undetected

gaseous component with the same distribution as the HI but substantially more mass. Implicit in this is that the dark matter be confined to a disk, which has the usual problems with disk instability (Ostriker & Peebles 1973). If instead the BDM is distributed in a halo, there is no reason to draw a connection between the shape of the HI disk and that of the total rotation curve.

We can test the notion of gas-scaling against the rotation curves of LSB galaxies. This sometimes works tolerably well, as long as one is free to adjust the scaling factor from galaxy to galaxy. However, it frequently fails to reproduce the shape of the rotation curves at all well. In Fig. 15, we show the *best* fit that can be obtained by this method to the best resolved LSB galaxy. The shape of the actual rotation curve is completely different from that predicted by the HI distribution. This is often true of the LSB data, so even though there may be some cases of HSB galaxies where the rotation curves are reasonably well predicted by the HI distribution, this simply is not the case in LSB galaxies. This removes a major argument in favor of BDM.

The various arguments in favor of BDM make no sense in the context of the LSB galaxy observations. This does not completely rule out the existence of BDM, or mean that we have discovered and cataloged every baryon in the universe. But it does make it very difficult to construct a sensible model with a dynamically important component of BDM.

In general, the arguments which favor BDM are based on the inferred coupling between dark and luminous matter. With this much we certainly concur: the two components must be intimately related (e.g., §6.2). Indeed, there does exist a unique analytic formalism relating the dynamics to the observed luminous mass distribution (papers II and III).

## 8. General Constraints on Baryon Fractions

There are a few interesting constraints that can be placed on the presence of dark matter completely irrespective of its composition. There is a wealth of data besides rotation curves which bear on the issue. These place both upper and lower limits on the extent and mass of dark matter halos, and sometimes provide measures of the actual baryon fraction.

Observations which place lower limits include the maximum radii to which rotation curves remain flat (Sancisi & van Albada 1987; Meurer et al. 1996), the timing argument in the local group (Kahn & Woltjer 1959; Peebles et al. 1989), the statistical motions of satellite galaxies at large separations from  $L^*$  galaxies (Zaritsky & White 1994), and QSO absorption lines which imply large halos with roughly flat rotation curves extending to very large radii (Barcons et al. 1995). Evidence which places upper limits on the extent of dark halos is more difficult to establish, but there is the very important result that overly massive halos suppress the formation of observed tidal tails (Dubinski et al. 1996). In addition, it might be possible to constrain the amount of dark matter allowed within the optical radius by disk stability constraints. Some dark matter is needed to stabilize disks (Ostriker & Peebles 1973), but too much inhibits features like spiral arms which stem from self gravity in the disk. This criterion has been used by Athanassoula et al. (1987) to

place minimum masses on disks in disk-halo decompositions. Finally, it now seems reasonably well established that actual baryon fractions can be measured in X-ray galaxy clusters so that the ratio of dark to luminous mass is known (White 1993; White & Fabian 1995; Evrard et al. 1996).

The most interesting (i.e., extreme) of these limits are shown in Fig. 16 and given in Table 5. Listed are the object, the type of data and analysis, the linear extent required of the dark matter halo (in both kpc and disk scale lengths where applicable), the observed mass to light ratio  $\Upsilon_o$ , the ratio of dark to luminous mass, the corresponding baryon fraction, and the source of the data. We have been as conservative as possible in assessing these limits; most of them are quite hard.

Listed first are those observations which place lower limits on the amount of dark matter required. The hardest of these limits come from the extended H I rotation curves of disk galaxies. These are observed to remain flat as far as observed, sometimes to very large radii. To calculate the limits, we have used the maximum disk case, attributing as much mass as possible to the luminous matter. The minimum required dark mass is then just  $V_c^2 R/G - \mathcal{M}_{bar}$ . NGC 3198 is a classic example of an HSB spiral with a rotation curve which remains flat to 11 scale lengths, nearly 3 times the extent of the bulk of the luminous mass. The dark halo must extend at least this far, and presumably much further since there is no hint of a turn down in  $V(R)$ . However, the required amount of dark mass is fairly modest:  $\mathcal{M}_{dark}$  exceeds the observed luminous mass  $\mathcal{M}_{bar}$  by only a factor of a few. Recently, Meurer et al. (1996) have been able to trace  $V(R)$  out to 22 scale lengths in the HSB dwarf NGC 2915. This extraordinary radius places interesting constraints, with the dark mass exceeding the luminous baryonic mass by at least a factor of 19. There are 4 LSB galaxies listed in Table 5; we have chosen the most extreme examples with  $\mathcal{M}_{dark}/\mathcal{M}_{bar} > 10$ . There are many more which are nearly as extreme (de Blok & McGaugh 1997). Even though  $V(R)$  is not measured to large  $R/h$  in LSB galaxies as in the above 2 examples, it should be obvious from Fig. 4 that LSB galaxies provide interesting limits in this way. The lowest surface brightness galaxies have  $\Upsilon_o > 30$ , so  $\mathcal{M}_{dark}/\mathcal{M}_{bar} > 10$  for  $\mathcal{M}_{bar}/L = 3$ . This is a fairly conservative number in the  $B$ -band;  $\Upsilon_* \approx 2$  is more realistic. We do not need to make any assumption about  $\Upsilon_*$  though: the dynamical mass of the baryonic disk is constrained by the rotation curve.

We stress that the limits obtained from the maximum disk decompositions of the rotation curves provide very hard lower limits on  $\mathcal{M}_{dark}/\mathcal{M}_{bar}$  and  $R_H$ . Maximum disk does not generally return realistic values for  $\Upsilon_*$ , especially in LSB galaxies (de Blok & McGaugh 1997). A more reasonable estimator based on disk velocity dispersions (Bottema 1993, 1997) gives nearly a factor of 2 less in HSB galaxies and even less in LSB galaxies. Also, we have of course not observed to the edge of the halo. It is difficult to construct a model in which the effects of an outer edge to the halo does not lead to observable consequences unless  $R_H > 2R_o$ . The point is that the limits in Table 5 are both hard and conservative. A more realistic estimate gives a result 3 or 4 times more extreme.

Aside from H I rotation curves, there are a number of other observations which place lower



limits on the extent of dark matter halos. Barcons et al. (1995) present observations of two systems with QSO absorption lines in ionized gas many tens of kpc from the centers of disk galaxies, very nearly along the major axis. The gas is apparently associated with the galaxies, though the geometry and orbital orientation are unknown. Nevertheless, nearly flat rotation seems to persist out to very large radii. If interpreted in the most obvious way, this implies limits even more extreme than those derived from bona-fide rotation curves.

On larger scales, the timing argument in the local group (e.g., Peebles et al. 1989) implies yet more dark matter. The same sort of result follows from the motions of satellite galaxies around  $L^*$  galaxies, which show no evidence of an edge to the halos to the largest scales probed,  $\gtrsim 200$  kpc (Zaritsky & White 1994; Zaritsky et al. 1997). Though statistical in nature, both of these approaches robustly require  $\Upsilon_o > 100$ . For  $\mathcal{M}_{bar}/L = 3$ , this means  $\mathcal{M}_{dark}/\mathcal{M}_{bar} > 33$ . This is generally consistent with the impression given by the rotation curves: dark matter halos are large and massive.

The lower limits just discussed are challenging to obtain. Perhaps even more difficult to acquire are upper limits on the extent of dark matter halos. Nevertheless, a few constraints can be placed. Recently, Dubinski et al. (1996) have pointed out that massive halos suppress the formation of tidal tails observed around merger remnants. This constrains the dark to luminous mass ratio rather severely; tidal features do not form unless  $\mathcal{M}_{dark}/\mathcal{M}_{bar} \lesssim 10$ . This upper limit is smaller than the hard lower limits imposed above,  $\mathcal{M}_{dark}/\mathcal{M}_{bar} > 20$ .

The results of Dubinski et al. (1996) are based on  $N$ -body simulations which one might simply choose to dismiss as model dependent. However, further modeling (Mihos et al. 1997) shows that there is no plausible variation of parameters which changes the essential result. There is a very good, simple reason for this. If dark matter halos are large and massive, the baryonic matter is buried at the bottom of a deep potential well. Even in a violent merger, the largest velocities imparted to some of the stars are insufficient to climb out of this potential well. This very effectively suffocates the formation of the large, linear features observed in merger remnants to extend over tens and sometimes even hundreds of kpc. Systems with  $\mathcal{M}_{dark}/\mathcal{M}_{bar} \gtrsim 10$  suppress such features before they get started.

Strictly speaking, it is the gradient of the potential which this modeling exercise constrains, not just the dark to luminous mass ratio (Mihos et al. 1997). It is possible to contrive very tenuous halo distributions which might weaken this limit, essentially by placing lots of mass at large radii where it does not participate in the merger dynamics. The tidal tails argument therefore provides the weakest of the limits discussed so far, and the only upper limit, so one might be tempted to equivocate. However, it does not appear that the argument can simply be dismissed. The limit it imposes is separated from the others by a factor of 2 and points in the *opposite* direction. Models contrived specifically to evade the tidal tails limit seem unlikely to satisfy other constraints.

Another way to constrain the ratio of halo to disk mass, at least within the radius of the disk, comes from disk stability. Purely Newtonian disks suffer from unchecked instabilities;

perturbations like bars grow exponentially and destroy the disk in a few dynamical times. The survival of spiral disks over a Hubble time requires some stabilizing influence. One possibility is to embed the disks in dynamically hot, spherical dark matter halos (Ostriker & Peebles 1973), though it should be noted that altering the effective force law can also have a stabilizing effect (Christodoulou 1991). The problem with dark matter halos is that they can provide too much stability. Observed features like bars and spiral arms occur because of self-gravity in the disk. If the halo is too dominant, this is negligible and one must invoke non-dynamical origins for the observed features. Athanassoula et al. (1987) used this fact to constrain  $\Upsilon_*$  in their rotation curve decompositions. In HSB galaxies, this gives reasonable results, the relevant effects being relatively small ( $\lesssim 50\%$  difference between the maximum disk and the minimum disk required to sustain spiral structure). Translating this into a limit on the dark halo mass within the radius of the optical disk gives  $\mathcal{M}_{dark}(R < 4h)/\mathcal{M}_{bar} \lesssim 3$  or 4.

LSB galaxies are so dark matter dominated, even within the optical extent of the disk, that features due to disk self gravity should simply not be evident (Mihos et al. 1997). The minimum disk required to form spiral features by the criteria of Athanassoula et al. (1987) exceeds the maximum disk allowed by the rotation curve (e.g., Quillen & Pickering 1997). Though rarely pretty grand design spirals, LSB galaxies do have spiral features (de Blok et al. 1995; McGaugh et al. 1995). This is not an isolated problem of a few strange morphologies;  $> 80\%$  of the 198 LSB galaxies in the primary list of Schombert et al. (1992) are spirals.

Again, one might be inclined to equivocate. Spiral structure is not well understood, and might not have an origin internal to disk dynamics at all. It is not likely that the spiral features can be attributed to interactions with companions, as LSB galaxies are usually very isolated (Bothun et al. 1993; Mo et al. 1994). The more extreme LSB galaxies have  $\mathcal{M}_{dark}(R < 4h)/\mathcal{M}_{bar} > 10$ , whereas dynamical spiral features seem to require  $\mathcal{M}_{dark}(R < 4h)/\mathcal{M}_{bar} < 4$ . Considerable work remains to be done to better quantify these effects, but the discrepancy is already large. There is a serious problem with invoking dark matter halos to stabilize disks if spiral structure is driven by disk self-gravity as often supposed.

So far we have only discussed limits which can be placed on the amount of dark matter required by various observations. Recently, it has become possible to estimate actual baryon fractions in X-ray clusters and groups of galaxies (White et al. 1993; White & Fabian 1995; Pildis et al. 1995). This procedure has a number of uncertainties, but the essential result seems to be quite robust (Evrard et al. 1996). This gives a surprisingly large amount of baryonic mass,  $f_b \approx 0.09$  for the value of the Hubble constant adopted here. This resides between the limits discussed above. The clusters give  $\mathcal{M}_{dark}/\mathcal{M}_{bar} \approx 10$ , while rotation curves, satellites and the local group all require  $\mathcal{M}_{dark}/\mathcal{M}_{bar} > 20$  and tidal tails imply  $\mathcal{M}_{dark}/\mathcal{M}_{bar} \lesssim 10$ .

At this juncture, it is unclear how to proceed. One option is to selectively disbelieve some combination of the results imposing these contradictory limits. Note that it is not possible to arrive at a single universal baryon fraction by dismissing a single limit; at least several observations

must be altered. Another option is to conclude that  $f_b$  varies arbitrarily from halo to halo. We could perhaps salvage a universal  $f_b$  by making some or all of the dark matter baryonic, and simply varying the fraction which becomes luminous. The distinction between these two latter possibilities is small. In both cases, we must randomly vary the amount of luminous matter in a way stipulated only by observation. Things that form tidal tails happen to have small halos. Galaxies with satellites happen to have large halos. The Tully-Fisher relation somehow manages to ignore these random, large fluctuations in the luminous to dark mass ratio and remain universal with little scatter. Structure formation theories lose all potential predictive power since  $f_b$  becomes a free parameter for each and every halo.

It is not clear whether the contradictory limits imposed by the various observations can be reconciled. Further work needs to concentrate on this point and on the fine-tuning problems that arise from the systematics of rotation curves. The current situation also poses a philosophical dilemma: what would be required to falsify the dark matter hypothesis?

We thank all the many, many people who have discussed and debated these issues with us with varying degrees of patience and credulity. We are particularly grateful to Renzo Sancisi and Vera Rubin for many enlightening conversations. Most of all, we would like to thank Thijs van der Hulst for his contributions to our work. We also thank Peter van Dokkum for the lively debate which clarified the virtues and vices of DD and SH, and brought out the implicit assumptions we all were making. We are also grateful to Chris Mihos, Roelof Bottema, Eric Schulman, Moti Milgrom, and the referee for their comments. We would both like to thank the Kapteyn Institute and the Department of Terrestrial Magnetism of the Carnegie Institution of Washington for their strong support and warm hospitality.

### A. Color Terms and the Slope of the Tully-Fisher Relation

In the discussion of the physical interpretation of the Tully Fisher relation (§5), we adopted the near infrared luminosity as an indicator of stellar mass. This results in a slope sometimes attributed to the viral theorem,

$$L \propto V_c^4. \tag{A1}$$

This particular slope is not specific to dark matter in general, as it depends on the assumptions which are necessarily made (§5).

Here we show that band pass dependent deviations of the slope from the adopted value have no significant impact on our discussion of the physical interpretation of the Tully Fisher relation. The full requirement on the relation between mass to light ratio, surface brightness, and luminosity imposed by the Tully-Fisher relation in any band pass  $j$  is

$$\Upsilon_j \propto \Sigma_j^{-1/2} L_j^{y_j/2} \tag{A2}$$

where  $y_j = (4 - x_j)/x_j$  measures the band pass dependent deviation of the slope of the Tully-Fisher relation from the adopted value of 4. This is a small effect compared to the fine balancing act which must be performed by  $\Upsilon$  and  $\Sigma$ .

Consider the residual color term between two bands  $j$  and  $k$ . The residual effect on the mass to light ratio is

$$\Delta \log \left( \frac{\Upsilon_k}{\Upsilon_j} \right) = \frac{4}{5x_j} \left[ (m_j - m_k) + \left( 1 - \frac{x_j}{x_k} \right) M_k \right] \quad (\text{A3})$$

where  $(m_j - m_k)$  is the color. For example, if  $x_V = 3$  and  $x_H = 4$ , this becomes

$$\Delta \log \left( \frac{\Upsilon_H}{\Upsilon_V} \right) = 0.27[(V - H) + 0.25M_H] \quad (\text{A4})$$

so a 1 mag. color change corresponds to a 0.27 dex shift in the ratio of  $\Upsilon$ , and 1 mag. in luminosity to a shift of only 0.07 dex.

Systematic changes in the slope of the Tully-Fisher relation with band pass can plausibly be attributed to modest systematic variation of the stellar population or extinction with luminosity. The observed trends operate in the sense expected for stellar populations (brighter galaxies tend to be redder) and the luminosity-metallicity relation (brighter galaxies should contain relatively more dust). These are small effects which have no real impact on the  $\Upsilon$ - $\Sigma$  relation. The increment for increment shift expected in the Tully-Fisher relation with surface brightness does not happen. This requires fine-tuning over nearly 5 magnitudes in  $\mu_0$  irrespective of the precise slope of the Tully-Fisher relation.

Table 1. Data

Galaxy	$M_B$	$\mu_0$	$h$	$V_c$	$i$	$\Upsilon_o$
F563–1	–17.3	23.5	4.3	111	25	36.6
F563–V2	–18.2	22.1	2.1	111	29	8.2
F568–1	–18.1	23.8	5.3	116	26	24.3
F568–3	–18.3	23.1	4.0	119	40	16.2
F568–V1	–17.9	23.3	3.2	124	40	20.8
F571–V1	–17.0	24.0	3.2	73	35	15.6
F574–1	–18.4	23.3	4.7	100	65	11.8
F583–1	–16.5	24.0	1.6	88	63	18.6
F583–4	–16.9	23.8	2.7	67	55	12.0
UGC 128	–18.8	24.2	9.2	130	55	28.8
UGC 6614	–20.3	24.5	15.8	204	36	30.2
DDO 154	–13.8	23.2	0.5	48	70	20.8
DDO 168	–15.2	23.4	0.9	55	58	13.5
NGC 55	–18.6	21.5	1.6	87	65	2.6
NGC 247	–18.0	23.4	2.9	108	72	12.8
NGC 300	–17.8	22.2	2.1	97	79	8.9
NGC 801	–21.7	21.9	12.0	222	81	7.4
NGC 1560	–15.9	23.2	1.3	79	75	21.2
NGC 2403	–19.3	21.4	2.1	136	67	4.4
NGC 2841	–21.7	21.1	4.6	323	69	6.0
NGC 2903	–20.0	20.5	2.0	201	78	4.8
NGC 2998	–21.9	20.3	5.4	214	63	2.7
NGC 3109	–16.8	23.1	1.6	67	62	8.2
NGC 3198	–19.4	21.6	2.6	157	64	6.7
NGC 5033	–20.2	23.0	5.8	222	30	14.3
NGC 5533	–21.4	23.0	11.4	273	75	14.1
NGC 5585	–17.5	21.9	1.4	92	76	7.1
NGC 6503	–18.7	21.9	1.7	121	66	4.9
NGC 6674	–21.6	22.5	8.3	266	78	8.1
NGC 7331	–21.4	21.5	4.5	241	65	4.3
UGC 2259	–17.0	22.3	1.3	90	63	10.0
UGC 2885	–22.8	21.9	13.0	298	68	5.3

Table 2. Other LSB Galaxies

Galaxy	Limitation
F561–1	$i < 25^\circ$
F563–V1	gross asymmetry
F564–V3	gross asymmetry
F565–V2	$V(R)$ still rising
F567–2	$i < 25^\circ$
F571–8	$i = 90^\circ$
F571–V2	no $B$ -band data
F574–2	$V(R)$ still rising
F577–V1	gross asymmetry
F579–V1	gross asymmetry
UGC 1230	$i < 25^\circ$
UGC 5005	no $B$ -band data
UGC 5209	unresolved
UGC 5750	no $B$ -band data
UGC 5999	no $B$ -band data

Table 3. Model

Test	DD	SH
Age	✓	?
$\phi(\mu_0)$	?	?
$\xi(r)$	✓	X
TF	X	✓
$V(R)$	✓	X

Table 4. Concentration

Model	$f_b = 0.09$	$V_{200} = 80$
SCDM	59	52
OCDM	9	8
$\Lambda$ CDM	12	11

Table 5. Limits on the Extent of Dark Halos

Object	Type	$R$ (kpc)	$R$ ( $h$ )	$\Upsilon_o$	$M_{dark}/M_{bar}$	$f_b$	Refs.
Lower Limits							
NGC 3198	H I $V(R)$	> 30	> 11	> 18	> 2.7	< 0.27	1
NGC 2915	H I $V(R)$	> 15	> 22	> 76	> 19	< 0.05	2
F568–V1	H I $V(R)$	> 19	> 6	> 41	> 11	< 0.08	3,4
F571–8	H I $V(R)$	> 15	> 4	> 49	> 20	< 0.05	3,4
UGC 5750	H I $V(R)$	> 21	> 6	> 10 <sup>a</sup>	> 11	< 0.08	3,5
UGC 5999	H I $V(R)$	> 15	> 3	> 35 <sup>a</sup>	> 11	< 0.08	3,5
1704+6068	QSO abs.	> 82	> 35	> 75	> 25 <sup>b</sup>	< 0.04	6
2135–1446	QSO abs.	> 64	> 16	> 123	> 41 <sup>b</sup>	< 0.03	6
Local Group	Timing	~ 700	...	> 100	> 33 <sup>b</sup>	< 0.03 <sup>b</sup>	7
Satellites	Statistical	> 200	...	> 100	> 33 <sup>b</sup>	< 0.03 <sup>b</sup>	8,9
Upper Limits							
Tidal Tails	Model	~ 100	...	< 30 <sup>b</sup>	< 10 <sup>c</sup>	> 0.09	10,11
Disk Stability	Theory	...	< 4	< 12 <sup>b</sup>	< 4 <sup>d</sup>	...	12,13
Measurement							
X-ray Clusters	$\beta$ -model	> 700	...	> 100 <sup>e</sup>	$11 \pm 4^f$	$0.09 \pm 0.03^f$	14,15

<sup>a</sup> $R$ -band:  $\Upsilon_o = \mathcal{M}/L_R$

<sup>b</sup>Assumes  $\mathcal{M}_{bar}/L = 3$

<sup>c</sup>Constrains total mass

<sup>d</sup>Constrains mass within disk

<sup>e</sup>Includes optical luminosity only

<sup>f</sup>Scaled to  $H_0 = 75 \text{ km s}^{-1} \text{ Mpc}^{-1}$ ; errors represent full range of data

References. — 1. Sancisi & van Albada 1987 2. Meurer et al. 1996 3. de Blok & McGaugh 1997 4. de Blok et al. 1996 5. van der Hulst et al. 1993 6. Barcons et al. 1995 7. Peebles et al. 1989 8. Zaritsky & White 1994 9. Zaritsky et al. 1997 10. Dubinski et al. 1996 11. Mihos et al. 1997a 12. Athanassoula et al. 1987 13. Mihos et al. 1997b 14. White & Fabian 1995 15. Pildis et al. 1995



## REFERENCES

- Aaronson, M., Huchra, J., & Mould, J. 1979, *ApJ*, 229, 1
- Alcock, C. et al. 1996, *ApJ*, 463, 67
- Andredakis, Y. C., & van der Kruit, P. C. 1992, *A&A*, 265, 396
- Ansari, R. et al. 1996, *A&A*, 314, 94
- Athanassoula, E., Bosma, A., & Papaioannou, S. 1987, *A&A*, 179, 23
- Bahcall, J. N., Flynn, C., & Gould, A. 1992, *ApJ*, 389, 234
- Barcons, X., Lanzetta, K. M., & Webb, J. K. 1995, *Nature*, 376, 321
- Barnes, J. & Efstathiou, G. 1987, *ApJ*, 319, 575
- Begeman, K. G., Broeils, A. H. & Sanders, R. H. 1991, *MNRAS*, 249, 523
- Bennett, C. L. et al. 1994, *ApJ*, 436, 423
- Bosma, A. 1981, *AJ*, 86, 1825
- Bothun, G. D., Impey, C. D., Malin, D. F., & Mould, J. R. 1987, *AJ*, 94, 23
- Bothun, G. D., Schombert, J. M., Impey, C. D., Sprayberry, D., & McGaugh, S. S. 1993, *AJ*, 106, 530
- Bottema, R. 1993, *A&A*, 275, 16
- Bottema, R. 1997, *A&A*, 328, 517
- Broeils, A. H. 1992, Ph.D. thesis, University of Groningen
- Burke, D. J., Collins, C. A., Sharples, R. M., Romer, A. K., Holden, B. P., & Nichol, R. C. 1997, *ApJ*, 488, 83
- Burstein, D., Rubin, V. C., Thonnard, N., & Ford, W. K. 1982, *ApJ*, 253, 70
- Carr, B. 1994, *ARA&A*, 32, 531
- Cen, R., & Ostriker, J. P. 1993, *ApJ*, 417, 415
- Christodoulou, D. M. 1991, 372, 471
- Cole, S. & Lacey, C. 1996, *MNRAS*, 281, 716
- Courteau, S. 1996, *ApJS*, 103, 363
- Copi, C., Schramm, D. N., & Turner, M. S. 1995, *Science*, 267, 192
- Dalcanton, J. J., Canizares, C. R., Granados, A., Steidel, C. C., & Stocke, J. T. 1994, *ApJ*, 424, 550
- Dalcanton, J. J., Spergel, D. N., & Summers, F. J. 1995, astro-ph/9503093
- Dalcanton, J. J., Spergel, D. N., & Summers, F. J. 1997, *ApJ*, 482, 659
- Davis, M., Nusser, A., & Willick, J. A. 1996, *ApJ*, 473, 22

- de Blok, W. J. G., & McGaugh, S. S. 1996, *ApJ*, 469, L89
- de Blok, W. J. G., & McGaugh, S. S. 1997, *MNRAS*, 290, 533
- de Blok, W. J. G., & McGaugh, S. S. 1998, in preparation (paper III)
- de Blok, W. J. G., McGaugh, S. S., & van der Hulst, J. M. 1996, *MNRAS*, 283, 18
- de Blok, W. J. G., van der Hulst, J. M., & Bothun, G. D. 1995, *MNRAS*, 274, 235
- de Jong, R. S. 1996a, *A&AS*, 118, 557
- de Jong, R. S. 1996b, *A&A*, 313, 45
- Donahue, M., Gioia, I., Luppino, G., Hughes, J. P., & Stocke, J. T. 1997, *astro-ph/9707010*
- Dubinski, J. 1994, *ApJ*, 431, 617
- Dubinski, J., & Carlberg, R. G. 1991, *ApJ*, 378, 496
- Dubinski, J., Mihos, J. C., & Hernquist, L. 1996, *ApJ*, 462, 576
- Efstathiou, G., & Jones, B. J. T. 1979, *MNRAS*, 186, 133
- Eisenstein, D. J., & Loeb, A. 1995, *ApJ*, 439, 520
- Evrard, A. E., Metzler, C. A., & Navarro, J. F. 1996, *ApJ*, 469, 494
- Fields, B. D., Kainulainen, K., Olive, K. A., & Thomas, D. 1996, *New Astronomy*, 1, 57
- Fisher, K. B., Davis, M., Strauss, M. A., Yahil, A., & Huchra, J. P. 1993, *ApJ*, 402, 42
- Flores, R. A., & Primack, J. R. 1994, *ApJ*, 427, L1
- Flores, R. A., Primack, J. R., Blumenthal, G. R., & Faber, S. M. 1993, *ApJ*, 412, 443
- Freeman, K. C. 1970, *ApJ*, 160, 811
- Frenk, C. S., Baugh, C. M., Cole, S. 1996, in *IAU Symposium No. 171: New Light on Galaxy Evolution*, eds. Bender, R. & Davies, R. L. (Dordrecht: Kluwer), 247
- Governato, F., Moore, B., Cen, R., Stadel, J., Lake, George, Quinn, T. 1997, *New Astr.*, 2, 91
- Hernquist, L. 1993, *ApJS*, 86, 389
- Heyl, J. S., Cole, Shaun, Frenk, Carlos S., & Navarro, J. F. 1995, *MNRAS*, 274, 755
- Hoffman, G. L., Salpeter, E. E., Farhat, B., Roos, T., Williams, H. & Helou, G. 1996, *ApJS*, 105, 269
- Huizinga, J. E., & van Albada, T. S. 1992, *MNRAS*, 254, 677
- Kahn, F. D., & Woljter, L. 1959, *ApJ*, 130, 705
- Kaiser, N. 1986, *MNRAS*, 222, 323
- Katz, N., & Gunn, J. E. 1991, *ApJ*, 377, 365
- Kent, S. M. 1987, *AJ*, 93, 816
- Kuijken, K. & Gilmore, G. 1989, *MNRAS*, 239, 605

- Lynden-Bell, D., Faber, S. M., Burstein, D. Davies, R. L., Dressler, A., Terlevich, R. J., & Wegner, G. 1988, *ApJ*, 326, 19
- Lake, G., & Feinswog, L. 1989, *AJ*, 98, 166
- McGaugh, S. S. 1992, Ph.D. thesis, University of Michigan
- McGaugh, S. S. 1994, *ApJ*, 426, 135
- McGaugh, S. S. 1996a, *MNRAS*, 280, 337
- McGaugh, S. S. 1996b, in *IAU Symposium No. 171: New Light on Galaxy Evolution*, eds. Bender, R. & Davies, R. L. (Dordrecht: Kluwer), 97
- McGaugh, S. S., & Bothun, G. D. 1994, *AJ*, 107, 530
- McGaugh, S. S., & de Blok, W. J. G. 1997, *ApJ*, 481, 689
- McGaugh, S. S., & de Blok, W. J. G. 1998, companion paper (paper II)
- McGaugh, S. S., Schombert, J. M. & Bothun, G. D. 1995, *AJ*, 109, 2019
- Merritt, D. 1997, *ApJ*, 486, 102
- Meurer, G. R., Carignan, C., Beaulieu, S. F., & Freeman, K. C. 1996, *AJ*, 111, 1551
- Mihos, J. C., Dubinski, J., & Hernquist, L. 1997, *astro-ph/9708009*
- Mihos, J. C., McGaugh, S. S., & de Blok, W. J. G. 1997, *ApJ*, 477, L79
- Mo, H. J., McGaugh, S. S., & Bothun, G. D. 1994, *MNRAS*, 267, 129
- Moore, B. 1994, *Nature*, 370, 629
- Mould, J. R., Akeson, R. L., Bothun, G. D., Han, M., Huchra, J. P., Roth, J., & Schommer, R. A. 1993, *ApJ*, 409, 14
- Navarro, J. F. 1996a, *astro-ph/9610188*
- Navarro, J. F. 1996b, in *IAU Symposium No. 171: New Light on Galaxy Evolution*, eds. Bender, R. & Davies, R. L. (Dordrecht: Kluwer), 255
- Navarro, J. F., Eke, V. R., & Frenk, C. S. 1996, *MNRAS*, 283, L72
- Navarro, J. F., Frenk, C. S., & White, S. D. M. 1996, *ApJ*, 462, 563
- Navarro, J. F., & Steinmetz, M. 1997, *ApJ*, 478, 13
- Ostriker, J. P. & Steinhardt, P. J. 1995, *Nature*, 377, 600
- Paczynski, B. 1996, *ARA&A*, 34, 419
- Peebles, P. J. E. 1971, *A&A*, 11, 377
- Peebles, P. J. E., Melott, A. L., Holmes, M. R., & Jiang, L. R. 1989, *ApJ*, 345, 108
- Pildis, R. A., Bregman, J. N., & Evrard, A. E. 1995, *ApJ*, 443, 514
- Pildis, R. A., Schombert, J. M., & Eder, J. 1997, *ApJ*, 481, 157

- Persic, M., Salucci, P., & Stel, F. 1996, MNRAS, 281, 27
- Pfenniger, D., Combes, F., & Martinet, L. 1994, A&A, 285, 79
- Prochaska, J. X., & Wolfe, A. M. 1997, ApJ, 487, 73
- Quillen, A. C., & Pickering, T. E. 1997, AJ, 113, 2075
- Renault, C. et al. 1997, A&A, 342, L69
- Rhee, M.-H. 1996, Ph.D. thesis, University of Groningen
- Richter, O.-G., & Sancisi, R. A&A, 290, 9
- Romanishin, W., Krumm, N., Salpeter, E. E., Knapp, G. R., Strom, K. M., & Strom, S. E. 1982, ApJ, 263, 94
- Rönnback, J., & Bergvall, N. 1994, A&A, 108, 193
- Rosati, P., Della Ceca, R., Norman, C., & Giacconi, R. 1998, ApJ, 492, L21
- Rubin, V. C., Ford, W. K., & Thonnard, N. 1980, ApJ, 238, 471
- Salpeter, E. E., & Hoffman, G. L. 1996, ApJ, 465, 595
- Sancisi, R. & van Albada, T. S. 1987, in IAU Symp. No. 117: Dark Matter in the Universe, eds. Knapp, G. & Kormendy, J. (Dordrecht: Reidel), 67
- Sanders, R. H. 1990, A&A Rev., 2, 1
- Scharf, C., Jones, L. R., Ebeling, H., Perlman, E., Malkan, M., Wegner, G. ApJ, ApJ, 477, 79
- Schombert, J. M., Bothun, G. D., Impey, C. D., & Mundy, L. G. 1990, AJ, 100, 1523
- Schombert, J. M., Bothun, G. D., Schneider, S. E., & McGaugh, S. S. 1992, AJ, 103, 1107
- Sprayberry, D., Bernstein, G. M., Impey, C. D., & Bothun, G. D. 1995b, ApJ, 438, 72
- Steinmetz, M., & Bartelmann, M. 1995, MNRAS, 272, 570
- Trimble, V. T. 1987, ARA&A, 25, 425
- Tully, R. B., & Fisher, J. R. 1977, A&A, 54, 661
- Tully, R. B., & Verheijen, M. A. W. 1997, ApJ, 484, 145
- Tyson, J. A., Wenk, R. A., & Valdes, F. 1990, ApJ, 349, L1
- van Albada, T. S., & Sancisi, R. 1986, Phil. Trans. R. Soc. A, 320, 447
- van der Hulst, J. M., Skillman, E. D., Smith, T. R., Bothun, G. D., McGaugh, S. S. & de Blok, W. J. G. 1993, AJ, 106, 548
- van der Kruit, P. C. 1987, A&A, 173, 59
- van der Marel, R. P. 1991, MNRAS, 253, 710
- Vogt, S. S., Mateo, M., Olszewski, E. W., & Keane, M. J. 1995, AJ, 109, 151
- White, D. A., & Fabian, A. C. 1995, MNRAS, 273, 72

- White, R. E., & Keel, W. C. 1992, *Nature*, 359, 129
- White, S. D. M., Navarro, J. F., Evrard, A. E. & Frenk, C. S. 1993, *Nature*, 366, 429
- Wiklind, T., Combes, F., & Henkel, C. 1995, *A&A*, 297, 643
- Zaritsky, D. & Lin, D. N. C. 1997, *AJ*, 114, 2545
- Zaritsky, D., Smith, R., Frenk, C., & White, S. D. M. 1997, *ApJ*, 478, 39
- Zaritsky, D. & White, S. D. M. 1994, *ApJ*, 435, 599
- Zwaan, M. A., van der Hulst, J. M., de Blok, W. J. G., & McGaugh, S. S. 1995, *MNRAS*, 273, L35
- Zwicky, F., & Humason, M. L. 1964, *ApJ*, 139, 269

Fig. 1.— The Tully-Fisher relation for spiral galaxies over a large range in surface brightness. The B-band relation is shown; the same result is obtained in all bands. In (a), the “authentic” Tully-Fisher relation is shown with the abscissa being the velocity width of the 21 cm line observed by single dish radio telescopes. Corrections have been applied as per Tully & Foqué (1985) as discussed by Zwaan et al (1995). In (b), the “intrinsic” Tully-Fisher relation is plotted with  $V_c$  measured from full rotation curves plotted along the abscissa. The velocity measurements in (a) and (b) are completely independent, and there is little overlap between the samples. The lines are fits to the data; though there is a perceptibly different slope, to a good approximation  $W_{20}^c$  measures  $\sim 2V_c$ . Open symbols in (a) are an independent sample (Broeils 1992) taken to define the Tully-Fisher relation (solid line). Solid symbols are galaxies binned by surface brightness: stars:  $\mu_0 < 22$ ; squares:  $22 < \mu_0 < 23$ ; triangles:  $23 < \mu_0 < 24$ ; circles:  $\mu_0 > 24$ . Clearly, galaxies fall on the same Tully-Fisher relation irrespective of surface brightness.

Fig. 2.— Log-log plots showing the shapes of the rotation curves of two galaxies, one of high surface brightness (NGC 2403; open circles) and one of low surface brightness (UGC 128; filled circles). The two galaxies have very nearly the same asymptotic velocity  $V_c$  and luminosity, as required by the Tully-Fisher relation. However, they have central surface brightnesses which differ by a factor of 13. Even though the asymptotic velocities are similar,  $V_c$  occurs at a very small radius in the high surface brightness galaxy, but not until a very large radius in the LSB galaxy. Indeed, the rotation curve of UGC 128 is still rising at the last measured point of NGC 2403, which occurs at  $R \approx 9h$ .

Fig. 3.— The radius of dark matter domination  $R_{2:1}$  in disk galaxies of different (a) absolute magnitude and (b) central surface brightness. Dark matter domination is defined to occur when the mass discrepancy reaches a factor of two, even attributing as much mass to the disk as possible (maximum disk). That is,  $R_{2:1}$  is the radius where  $\mathcal{M}_T(R_{2:1})/\mathcal{M}_{disk}(R_{2:1}) \geq 2$ . Bright galaxies do not require much dark matter until quite large radii, whereas dim galaxies are dark matter dominated down to nearly  $R = 0$ . The mass discrepancy does not set in at any particular length scale.

Fig. 4.— The observed dynamical mass to light ratio  $\Upsilon_o$  (in  $\mathcal{M}_\odot/L_\odot$ ) plotted against a) luminosity, b) central surface brightness, and c) scale length. Error bars are plotted for a nominal inclination uncertainty of  $\sigma_i = 3^\circ$ . The very strong correlation in (b) is related to the Tully-Fisher relation (Zwaan et al. 1995) and can not be a selection effect.

Fig. 5.— The residuals about the Tully-Fisher relation as a function of surface brightness. The residual in luminosity is shown in (a), while that in velocity is shown in (b). The triangles are data where only the linewidth  $W_{20}^c$  has been measured while the circles are galaxies with  $V_c$  measured from a full rotation curve. Also shown as solid lines are the prior expectations for the relation between rotation luminosity or velocity and surface brightness for a fixed mass to light ratio. More diffuse, lower surface brightness galaxies require a higher mass and luminosity to achieve the same rotation velocity, or should peak at much lower velocities at the same mass. Though these statement

follow directly from  $V^2 = GM/R$  and the assumption of constant  $\Upsilon_o$ , neither are true — galaxies rigorously adhere to the Tully-Fisher relation (dashed lines) rather than following the expected trend (solid lines).

Fig. 6.— The fraction of baryonic mass in the form of stars  $f_* = \mathcal{M}_*/\mathcal{M}_b$  plotted against  $\Sigma_0$  (see McGaugh & de Blok 1996). There is a relation:  $f_* \propto \Sigma_0^{0.17}$ , but this is not sufficient to explain the  $\Upsilon_o$ - $\Sigma_0$  relation.

Fig. 7.— The  $\Upsilon_o$ - $\mu_0$  relation, with and without gas. The solid triangles include all mass within  $R_o = 4h$  (identical to Fig. 4b), while the open squares are the same quantity with the gas mass subtracted ( $\mathcal{M}_o^c = R_o V_c^2 G^{-1} - 1.4\mathcal{M}_{HI}$ ; the factor 1.4 is the standard correction for helium and metals.) The downward apex of each triangle points at the corresponding square for the same galaxy. Correcting for  $f_*$  has no impact on the  $\Upsilon_o$ - $\mu_0$  relation other than a very small downwards shift.

Fig. 8.— The surface brightness distribution (data points from various sources) together with the distribution expected from the variation of spin parameters. Solid line: Efstathiou & Jones (1979). Dashed line: Eisenstein & Loeb (1995). Theory predicts a very broad distribution with curvature inconsistent with observations. Worse, a cut-off must be inserted by hand to reconcile the high surface brightness end of  $\phi(\mu_0)$ .

Fig. 9.— Toy galaxy model rotation curves with  $V$  and  $R$  in normalized physical units. Each panel represents the expectations of the simple models described in the text. The dashed line is the contribution of the halo and the dotted line the contribution of the disk to the total rotation curve (solid line). Inset in each panel is a schematic representation of the model. Top panels are a fiducial HSB galaxy of high surface density residing in a high density halo. Lower panels are the expectations for LSB galaxies in two scenarios. On the left is the “density begets density” (DD) hypothesis with a diffuse LSB galaxy residing in a diffuse halo. On the right is the “Same Halo” (SH) case with a diffuse LSB galaxy extending out to near the edge of a dense halo. The expected shapes of the rotation curves are strikingly different:  $V(R)$  rises slowly and does not reach the same  $V_c$  as an HSB of the same mass in the DD case, while in the SH case this happens after a rapid rise.

Fig. 10.— The model LSB galaxy rotation curves from Fig. 9 confronted with data for galaxies of the appropriate surface brightness. Both models fail to predict the shapes of the actual rotation curves. These rise gradually as expected in the DD model, but reach a  $V_c$  dictated by the Tully-Fisher relation as expected in the SH model.

Fig. 11.— The relative luminosity density of disk galaxies  $J(\mu_0)$  as a function of surface brightness, as predicted by Dalcanton et al. (1997; line) and as observed (data as per Fig. 8; see McGaugh 1996).

Fig. 12.— The rate of rise of disk galaxy rotation curves as measured by the radius  $R_{34}$  where

$V(R_{34}) = {}^{3/4}V_c$ . (a)  $R_{34}/h$  vs. absolute magnitude and (b)  $R_{34}/h$  vs. disk central surface brightness. Only well resolved galaxies (at least 8 beams/diameter) are plotted. Bright galaxies have rapidly rising rotation curves, with  $V(R)$  frequently reaching  ${}^{3/4}V_c$  before one scale length. Dimmer galaxies have rotation curves which rise more gradually, sometimes not reaching  ${}^{3/4}V_c$  for three scale lengths. Also plotted are the predictions of the model of Dalcanton et al. (1997) for no luminosity-surface brightness correlation (solid line) and for  $L \propto \Sigma_0^{1/3}$  as they predict (dashed line). These predictions are obtained from their Fig. 1 and depend on two parameters, the halo mass  $\mathcal{M}_H$  and the spin parameter  $\lambda_s$ . Points along the lines are labeled by  $\log(\mathcal{M}_H)$  (in solar masses) in (a) and by  $\lambda_s$  in (b).

Fig. 13.— The predictions of Cen & Ostriker (1993) confronted with the data. The halo mass (a) and the cold gas mass (b) are shown as a function of stellar mass. The solid line represents the mean prediction while the dashed line shows the expected  $1\sigma$  dispersion. The squares in (a) are the data discussed here. The circles in (b) are data for spiral galaxies from McGaugh & de Blok (1997) while the triangles are data for elliptical galaxies from Wiklund et al. (1995). Cen & Ostriker (1993) predict far too strong a deviation from constant  $\mathcal{M}_T/\mathcal{M}_*$  in (a) (the dotted line is drawn for  $f_b = 0.05$ ). For the cold gas mass in (b), the prediction fares even worse. Too little cold gas is retained in galaxies at the present epoch, the slope of the predicted trend is orthogonal to the data, and the gas content of bright galaxies is off by five orders of magnitude.

Fig. 14.— The rotation curve of F583–1 compared with the form predicted for appropriate CDM halos (Navarro et al. 1996). The solid points are the observed rotation curve, while the open points are the rotation curve of the dark matter with the baryonic component subtracted from the total. The open points have been offset slightly in  $R$  for clarity, as the baryons contribute very little at any radii. Lines show the predictions of various cosmologies (Table 4) assuming (a)  $f_b = 0.09$ , the value indicated by clusters, and (b)  $V_{200} = 80 \text{ km s}^{-1}$  (i.e., a Tully-Fisher normalization which ignores the consequences for the baryon fraction.) None of the predictions are satisfactory, so in (c) we test whether any Navarro et al. (1996) profile can fit the observations, regardless of cosmology. Even treating both  $c$  and  $V_{200}$  as completely free parameters, no fit can be obtained. CDM predicts the wrong shape for galaxy halo density profiles.

Fig. 15.— The best fit we could attain for the rotation curve of a well resolved LSB galaxy, F583–1, by scaling the contribution of the H I component. The stars are assumed to contribute maximally, but this matters little to the fit. Clearly, there is no scaling which reproduces the shape of the observed rotation curve. Though the H I distribution may be a good indicator of the shape of the rotation curves in some HSB galaxies, it generally is not in LSB galaxies. This nullifies one of the arguments in favor of baryonic dark matter.

Fig. 16.— A graphical representation of the limits from Table 5. One would expect a universal baryon fraction, but no such value emerges unless only a small subset of the data are considered (e.g., clusters of galaxies). When all data are considered, one finds many contradictory measurements and nonoverlapping limits. Note that even within the same type of object, contradictory limits



occur. In disk galaxies, flat rotation curves require a lot of dark matter, while disk stability prefers a more moderate amount. For groups of galaxies, the Local Group requires much more dark matter than is measured in external groups. A broad distribution of baryon fractions seems to be required, but this contradicts the small scatter in the Tully-Fisher relation.

Figure 1

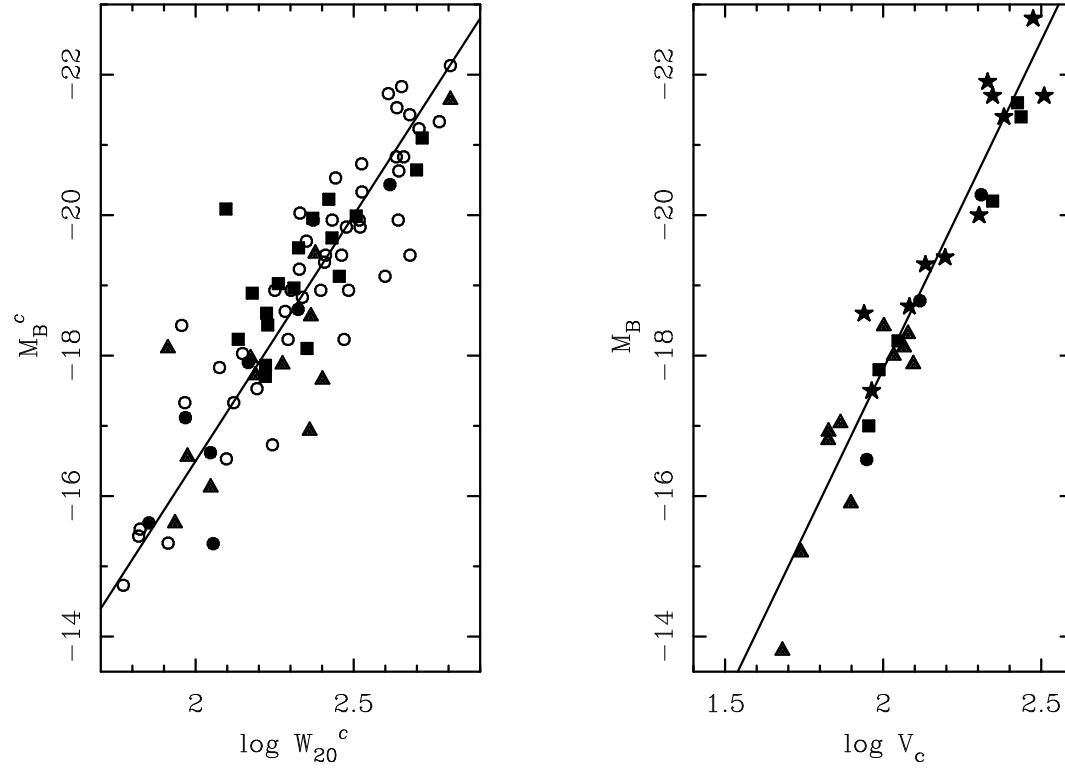


Figure 2

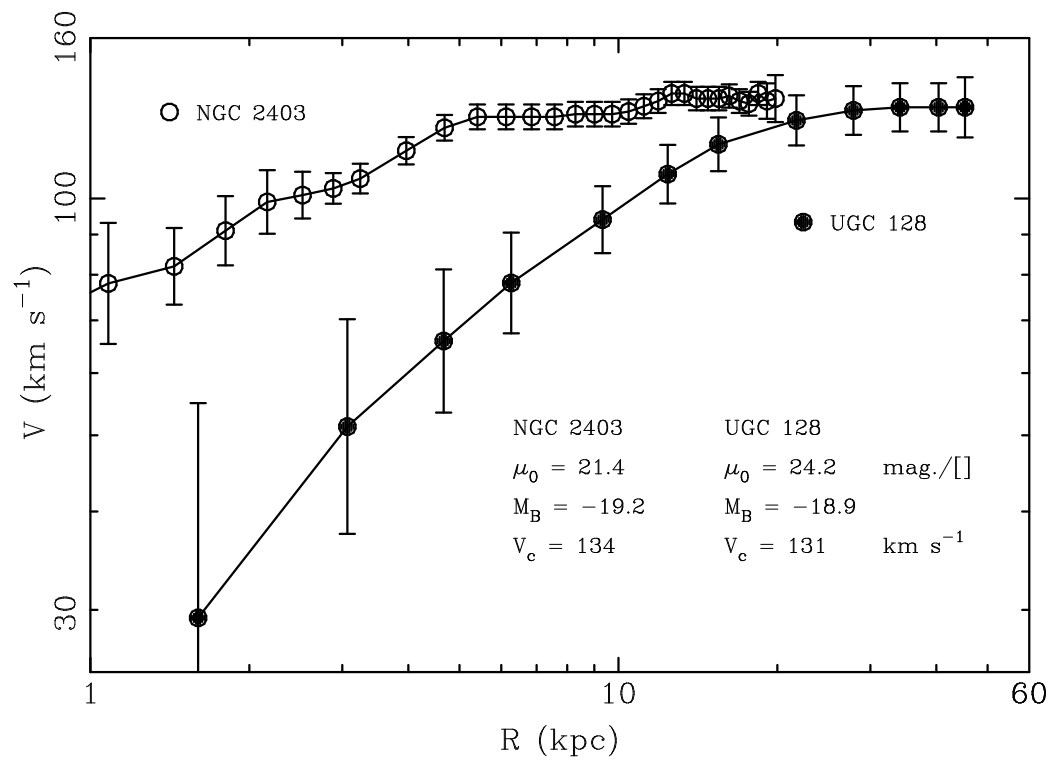


Figure 3a

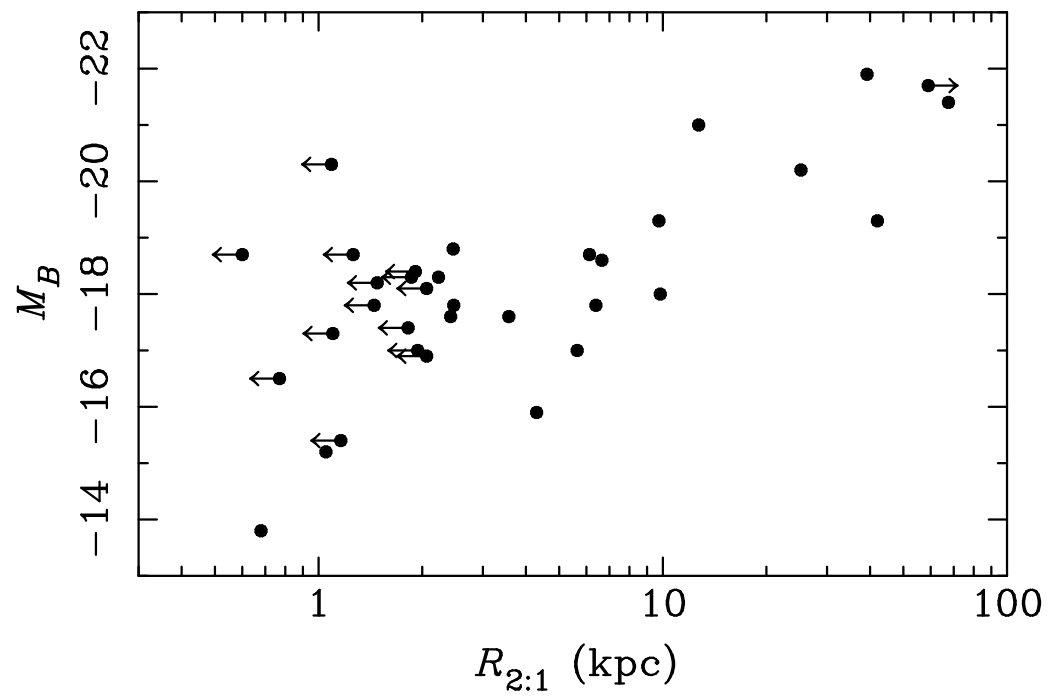


Figure 3b

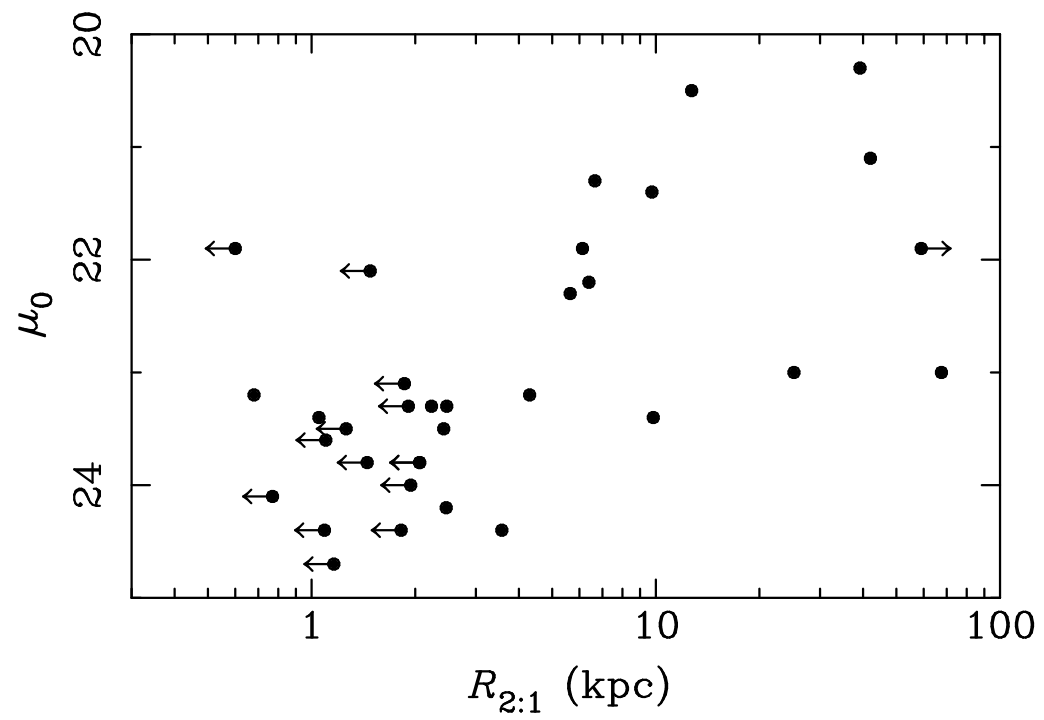


Figure 4a

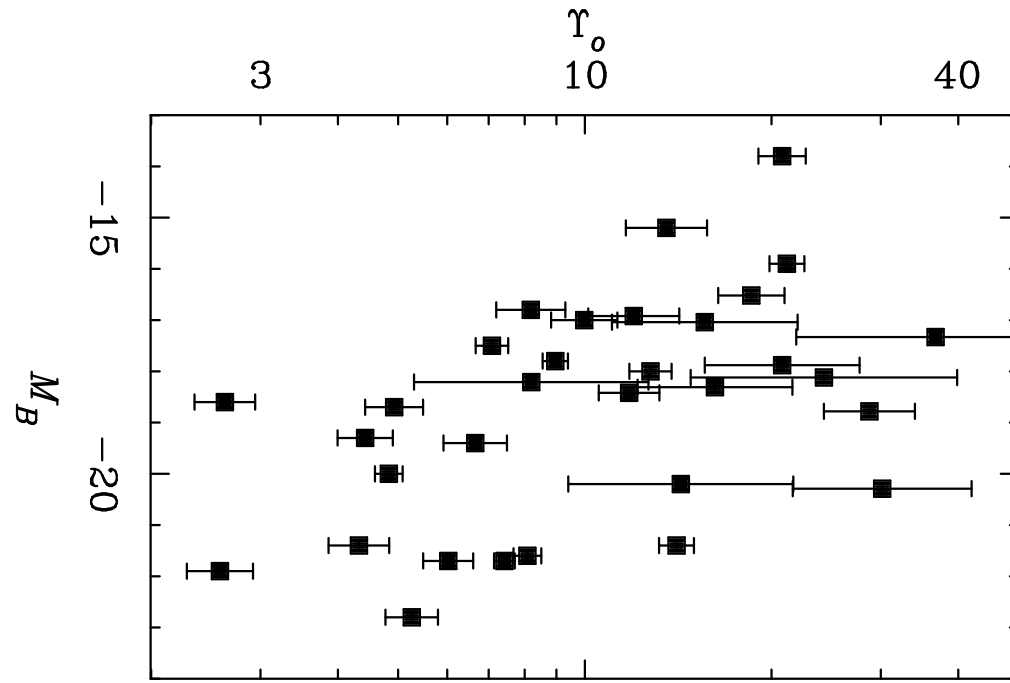


Figure 4b

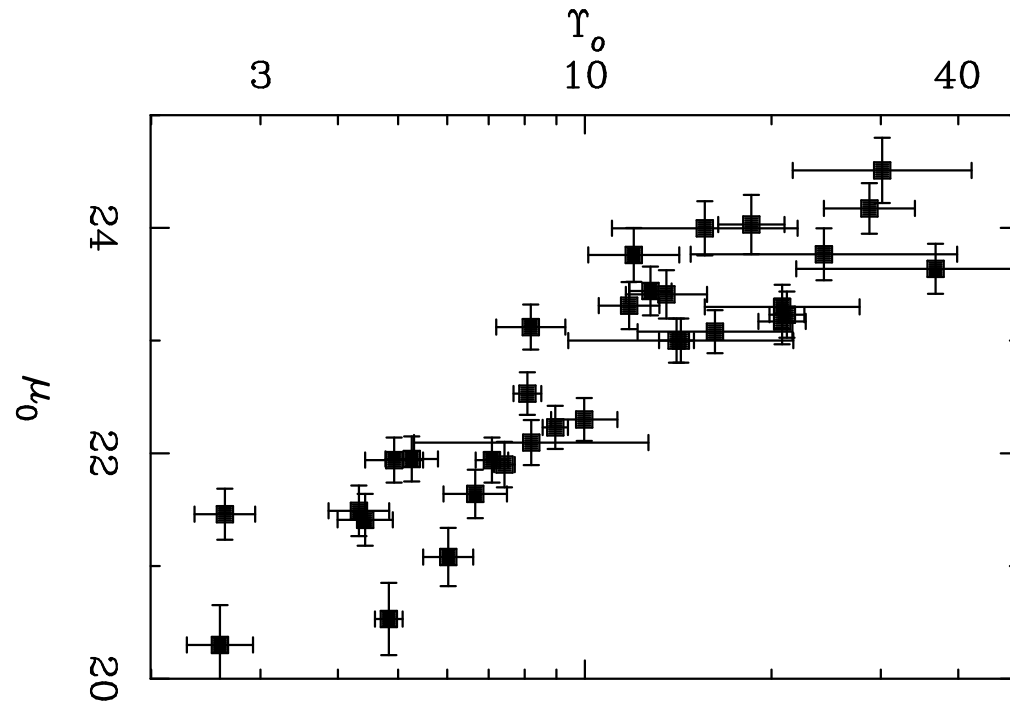


Figure 4c

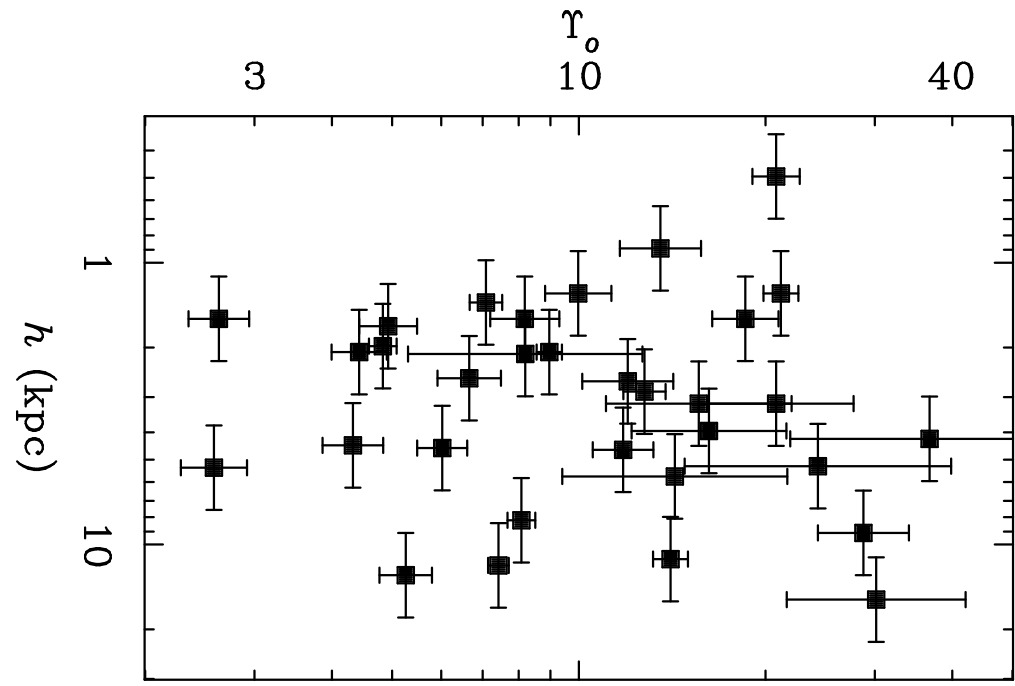




Figure 5

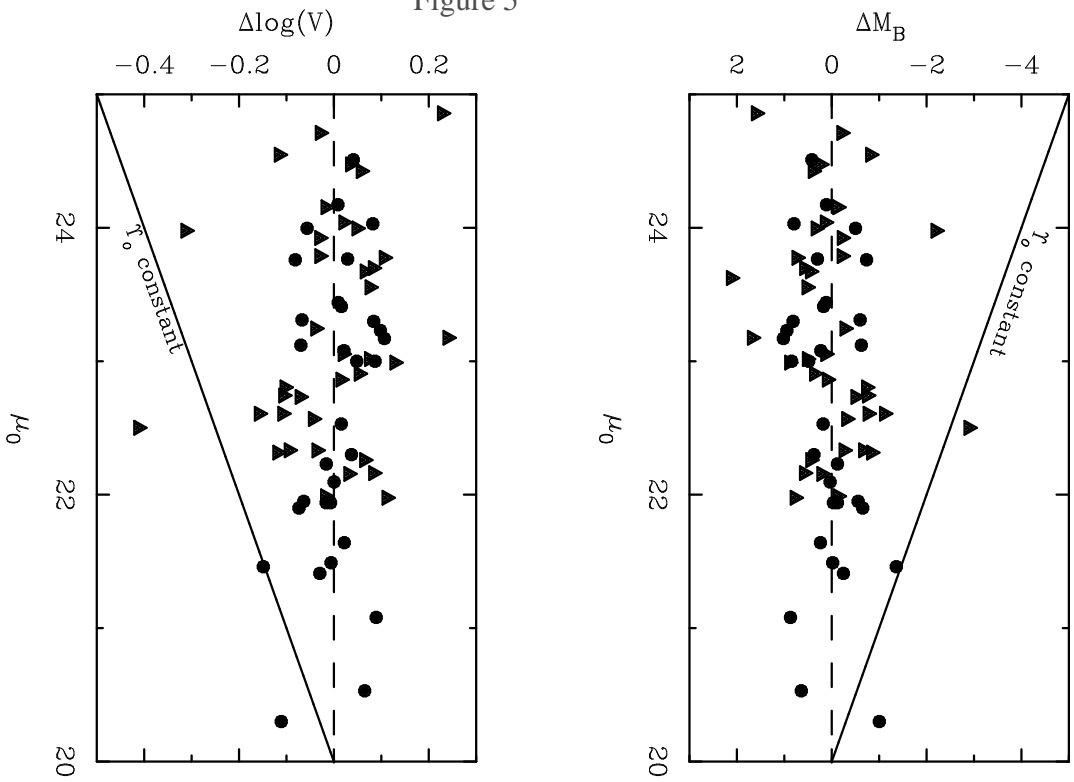


Figure 6

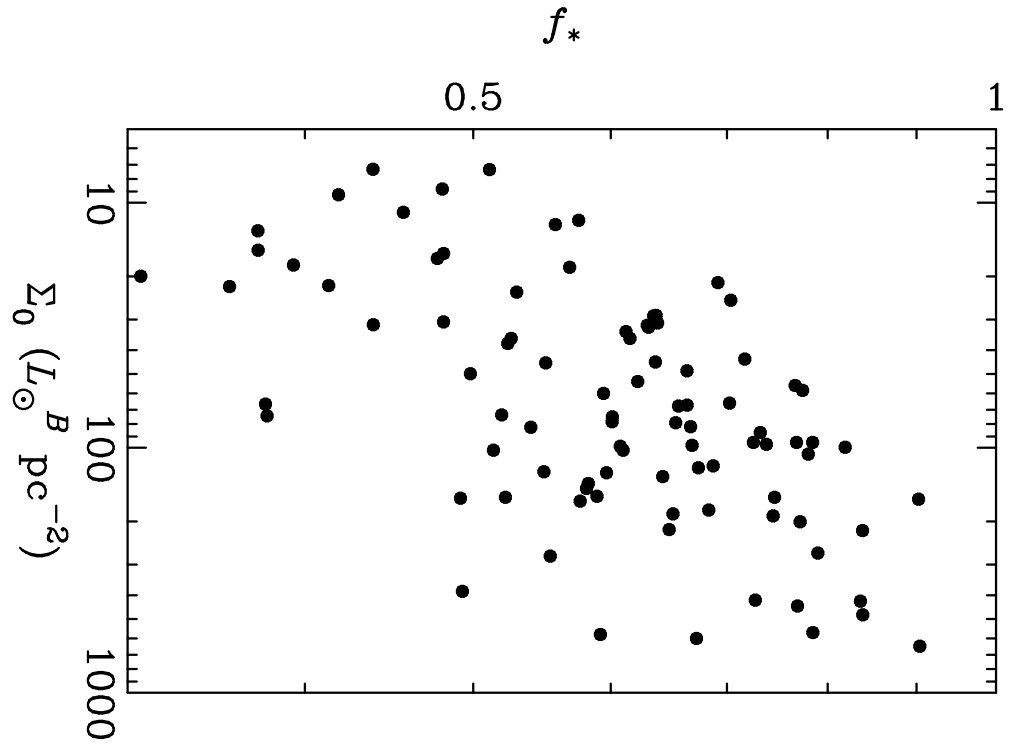


Figure 7

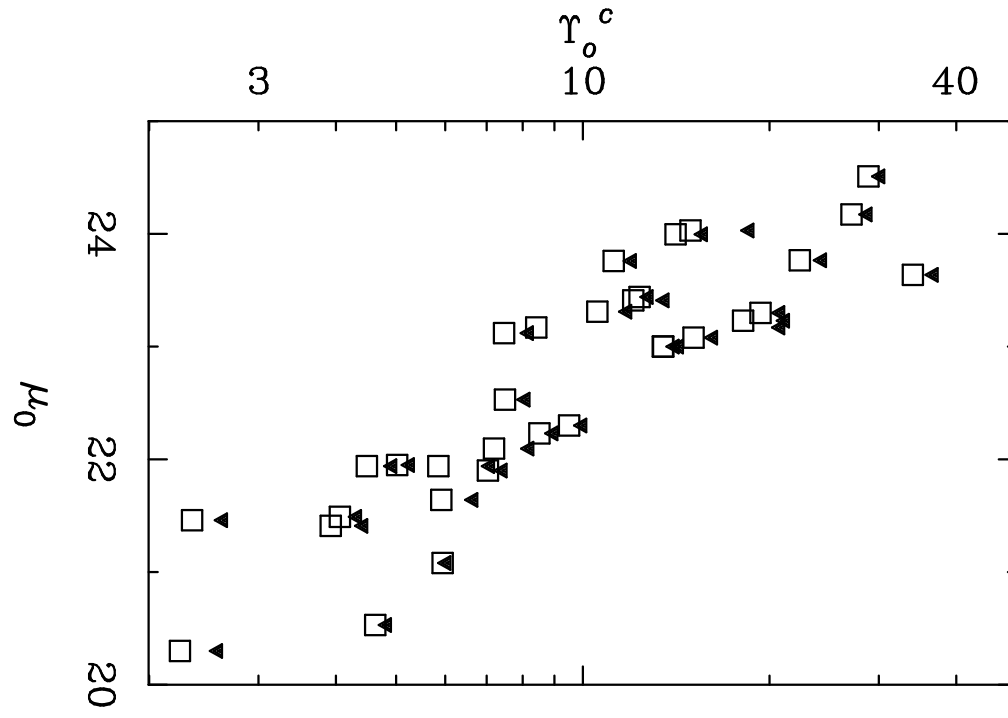


Figure 8

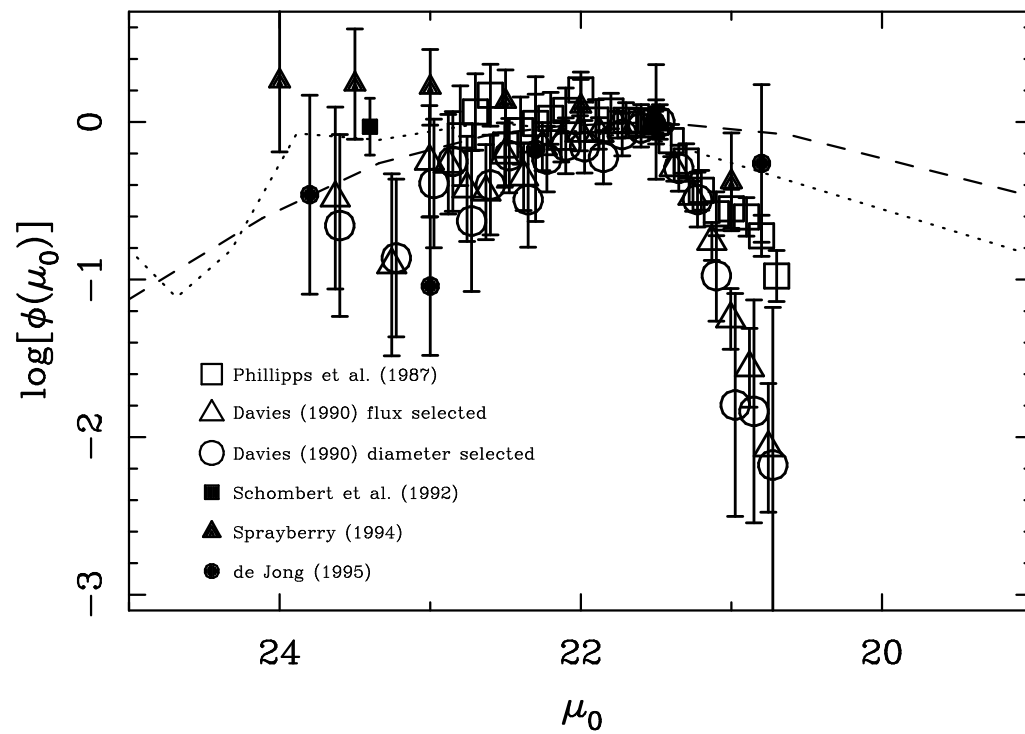


Figure 9

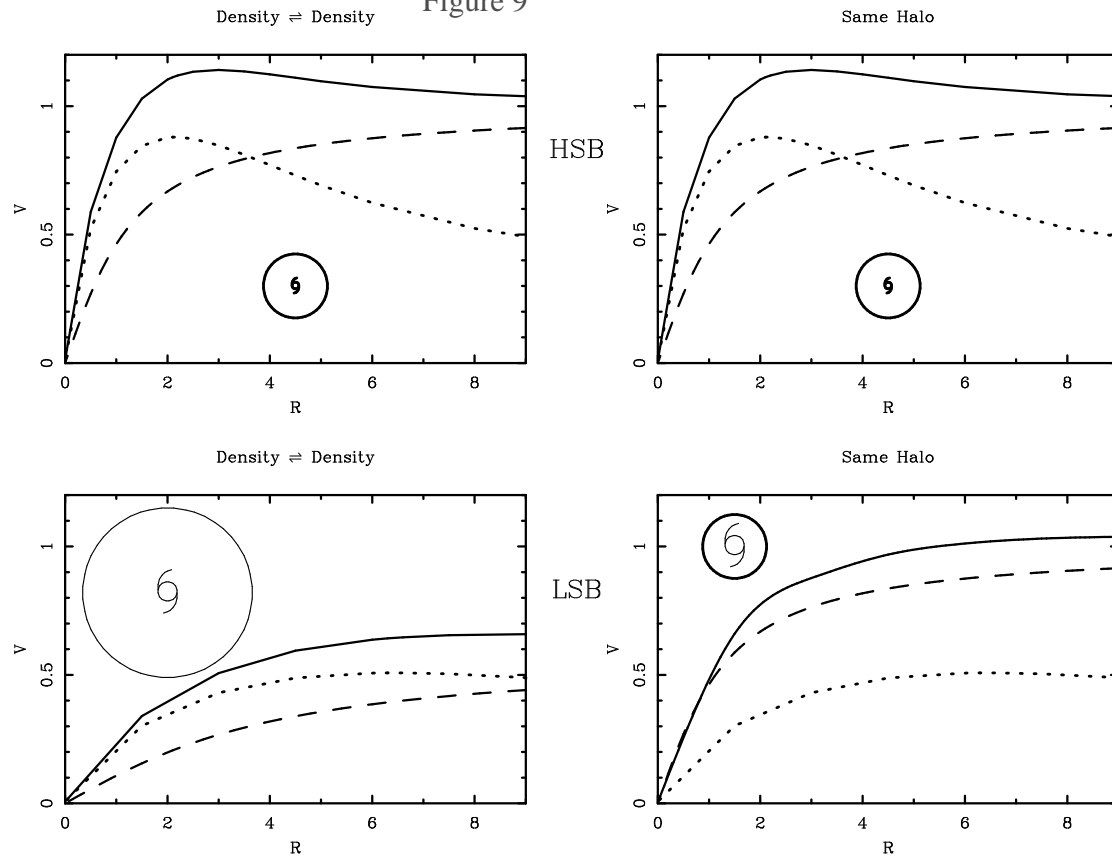


Figure 10

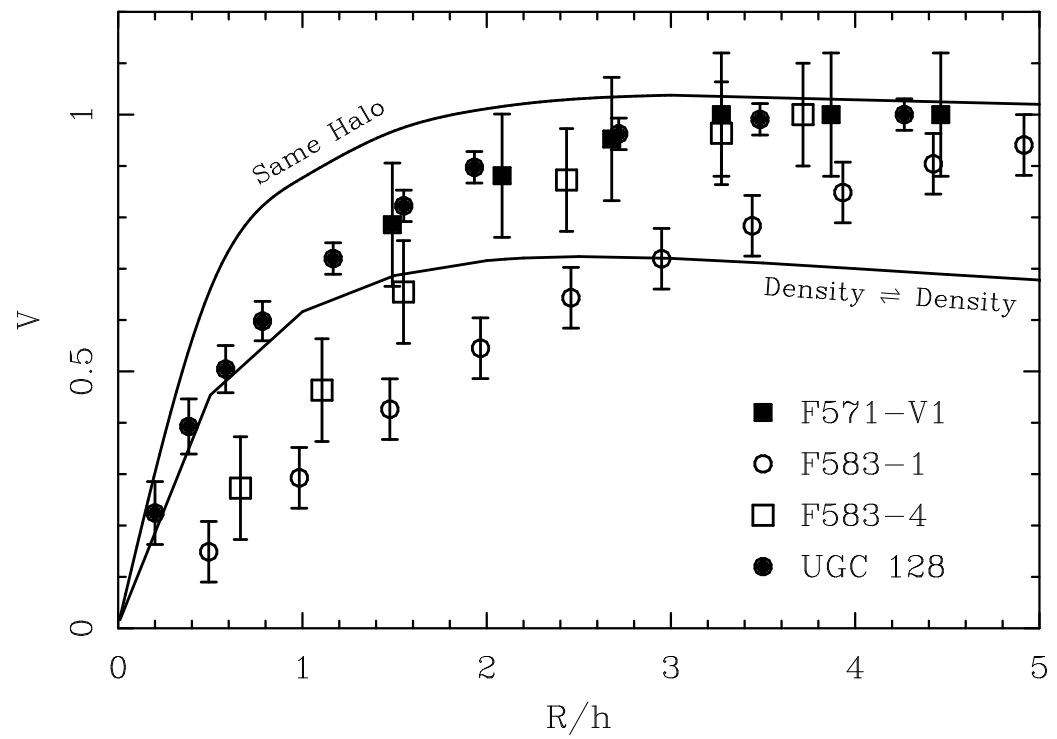


Figure 11

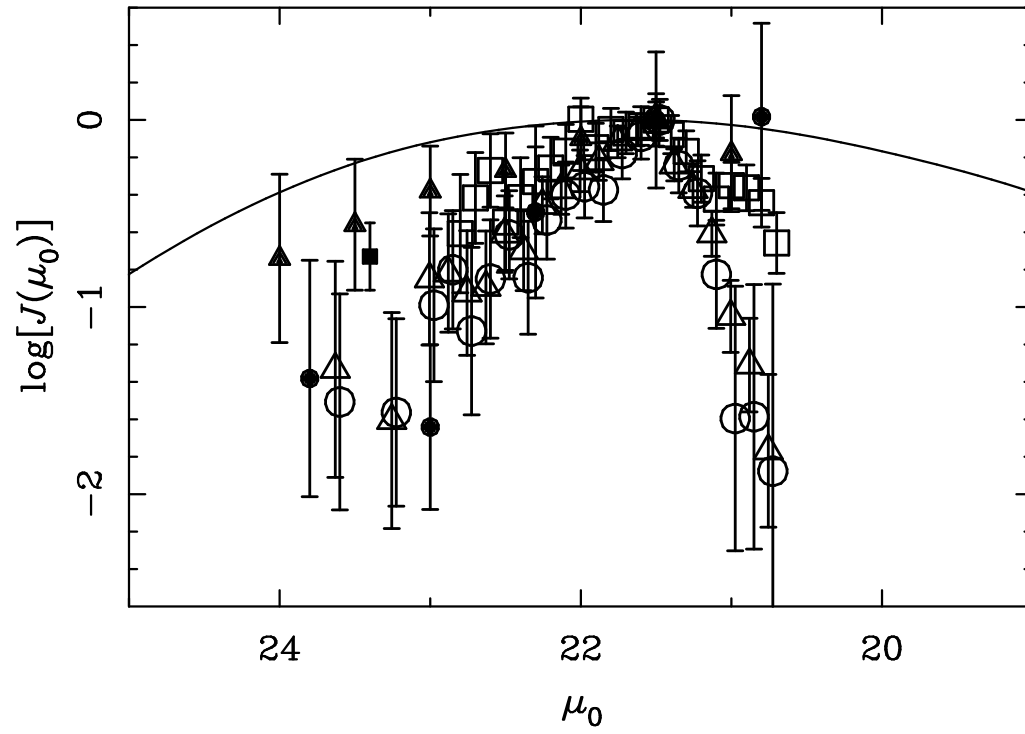


Figure 12a

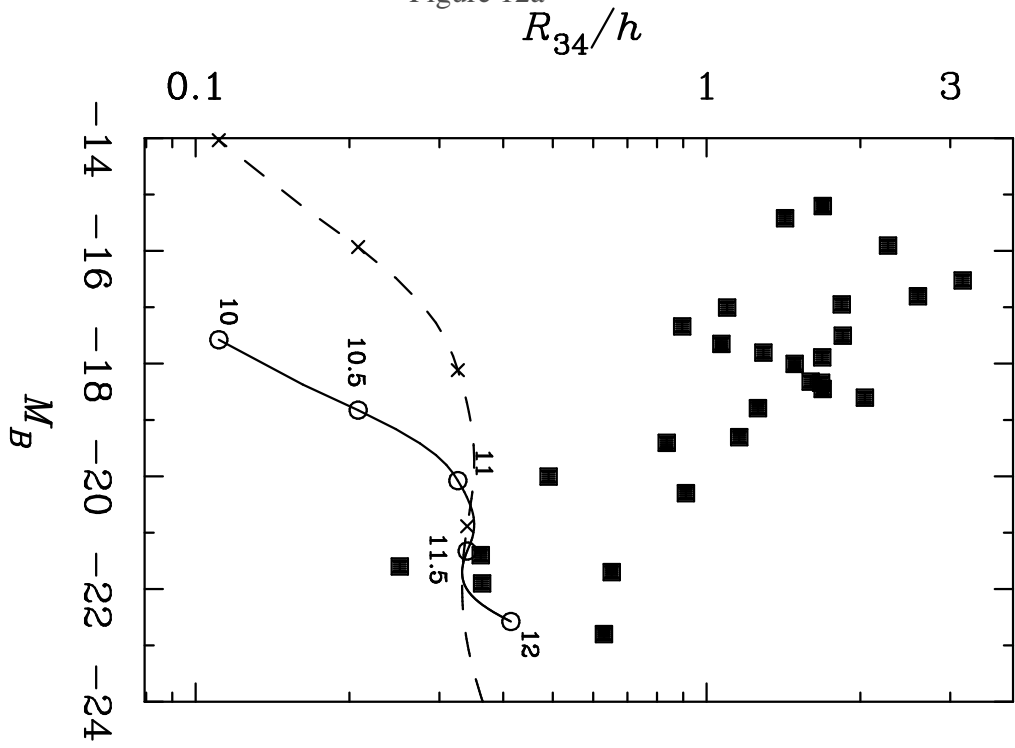




Figure 12b

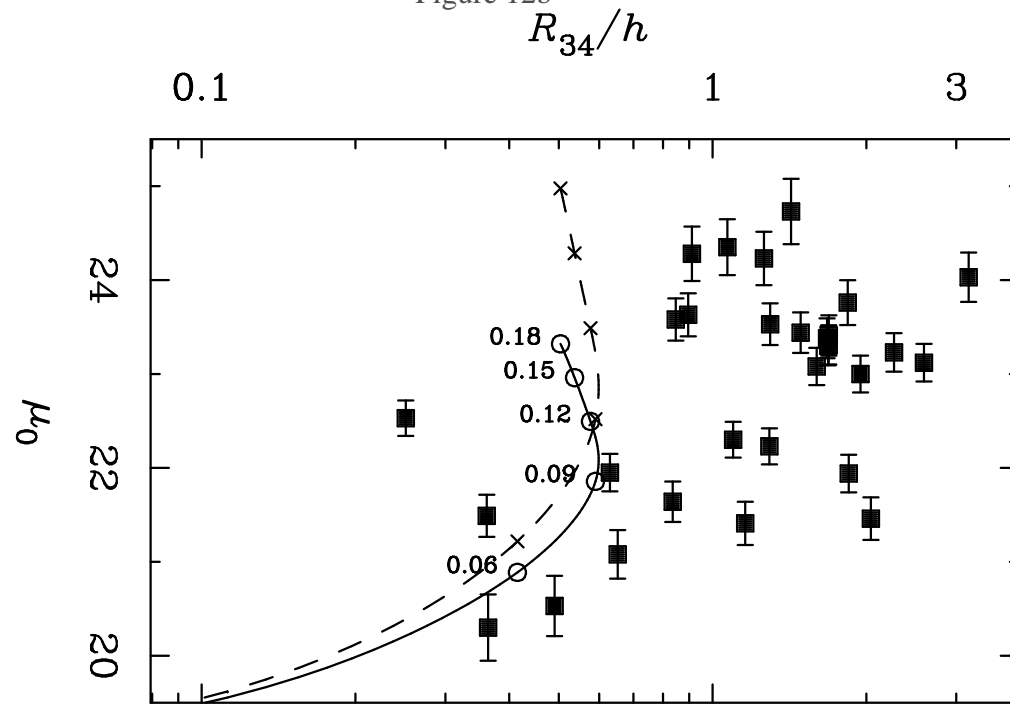


Figure 13a

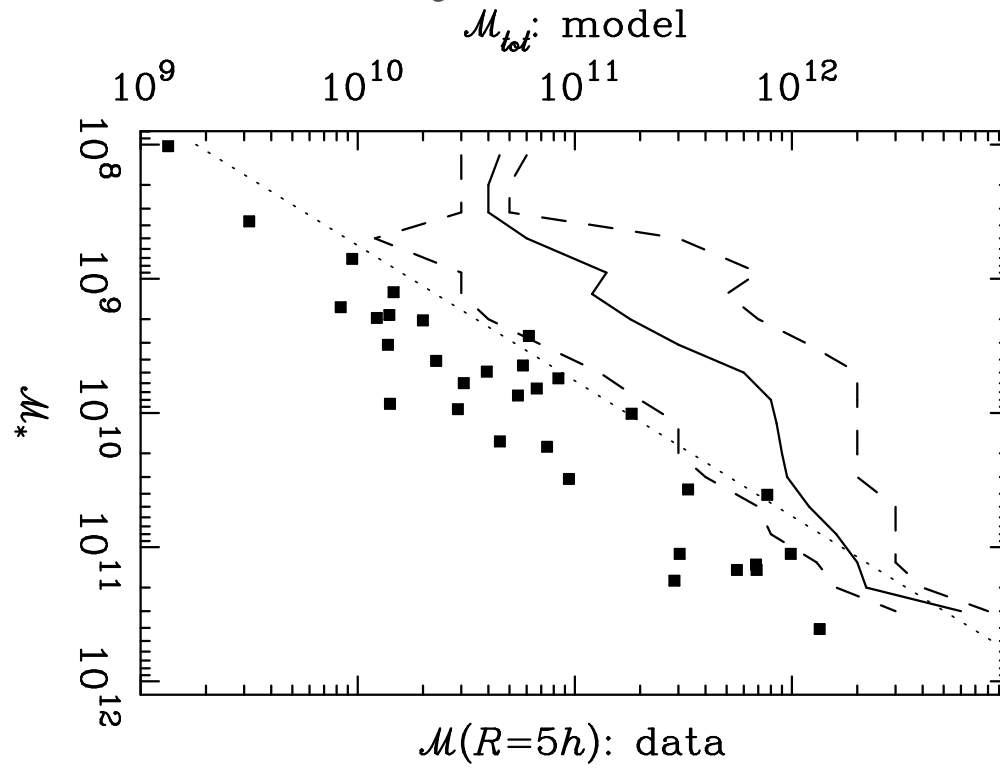


Figure 13b

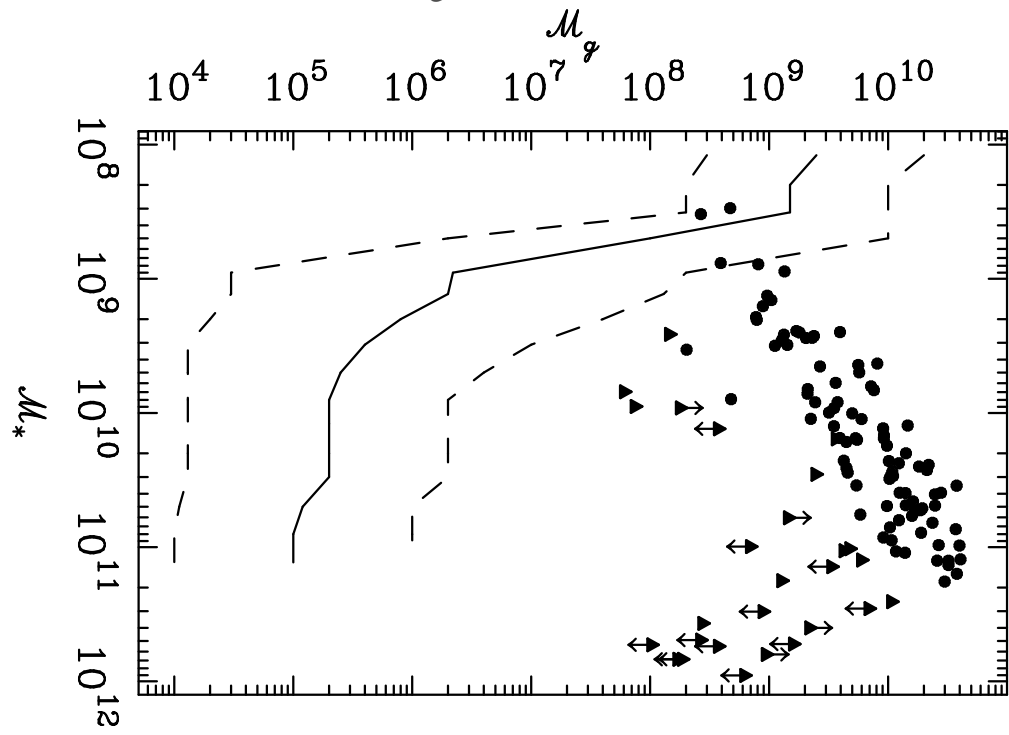


Figure 14a

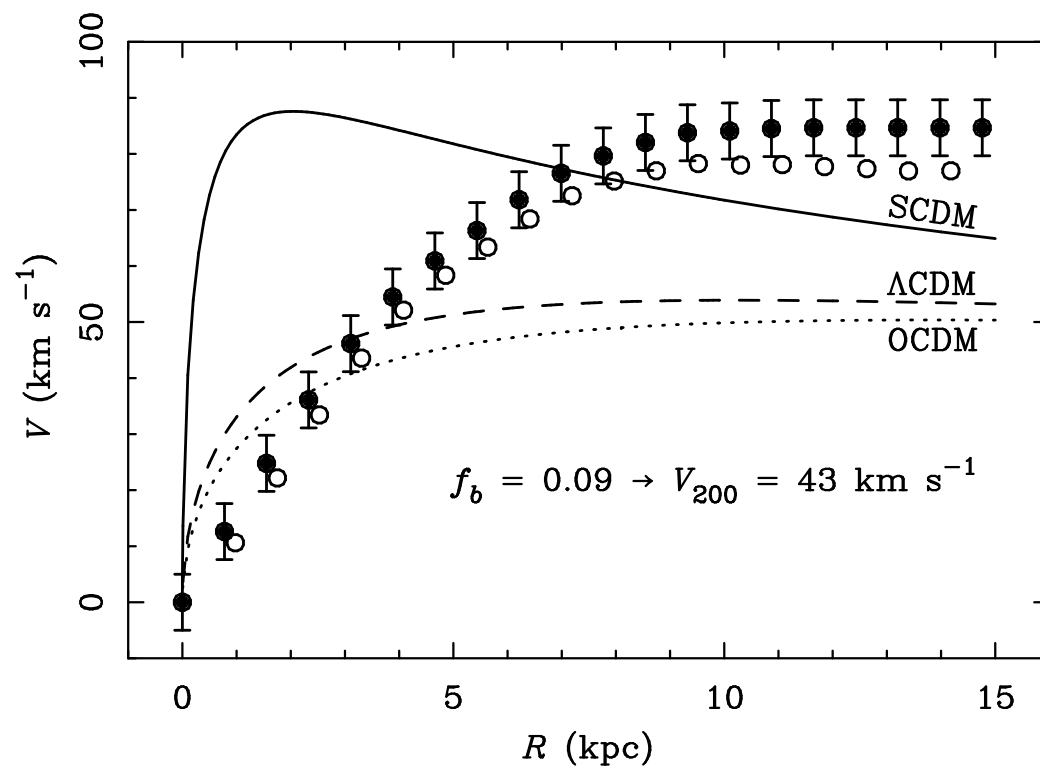


Figure 14b

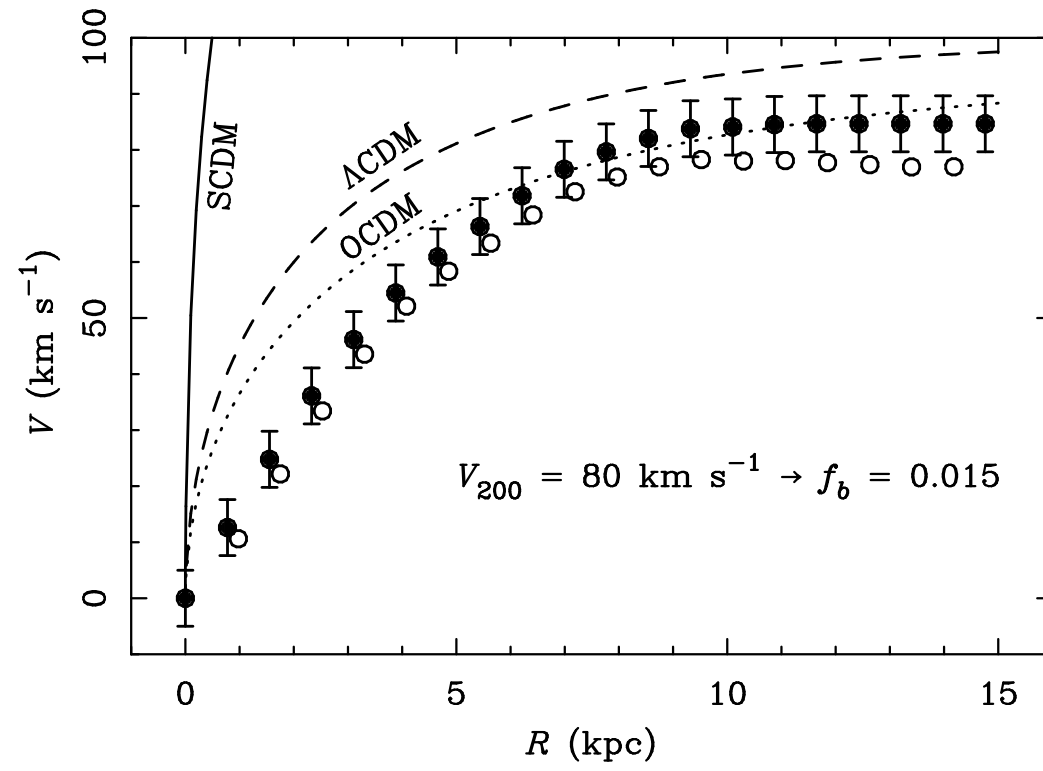
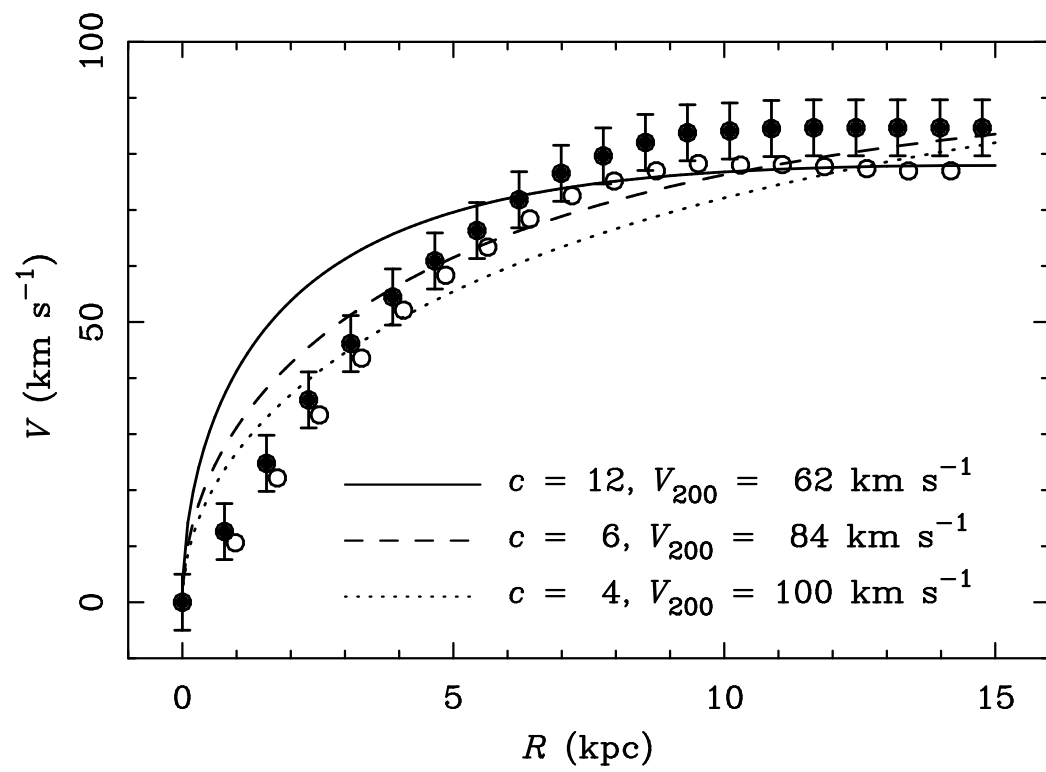


Figure 14c



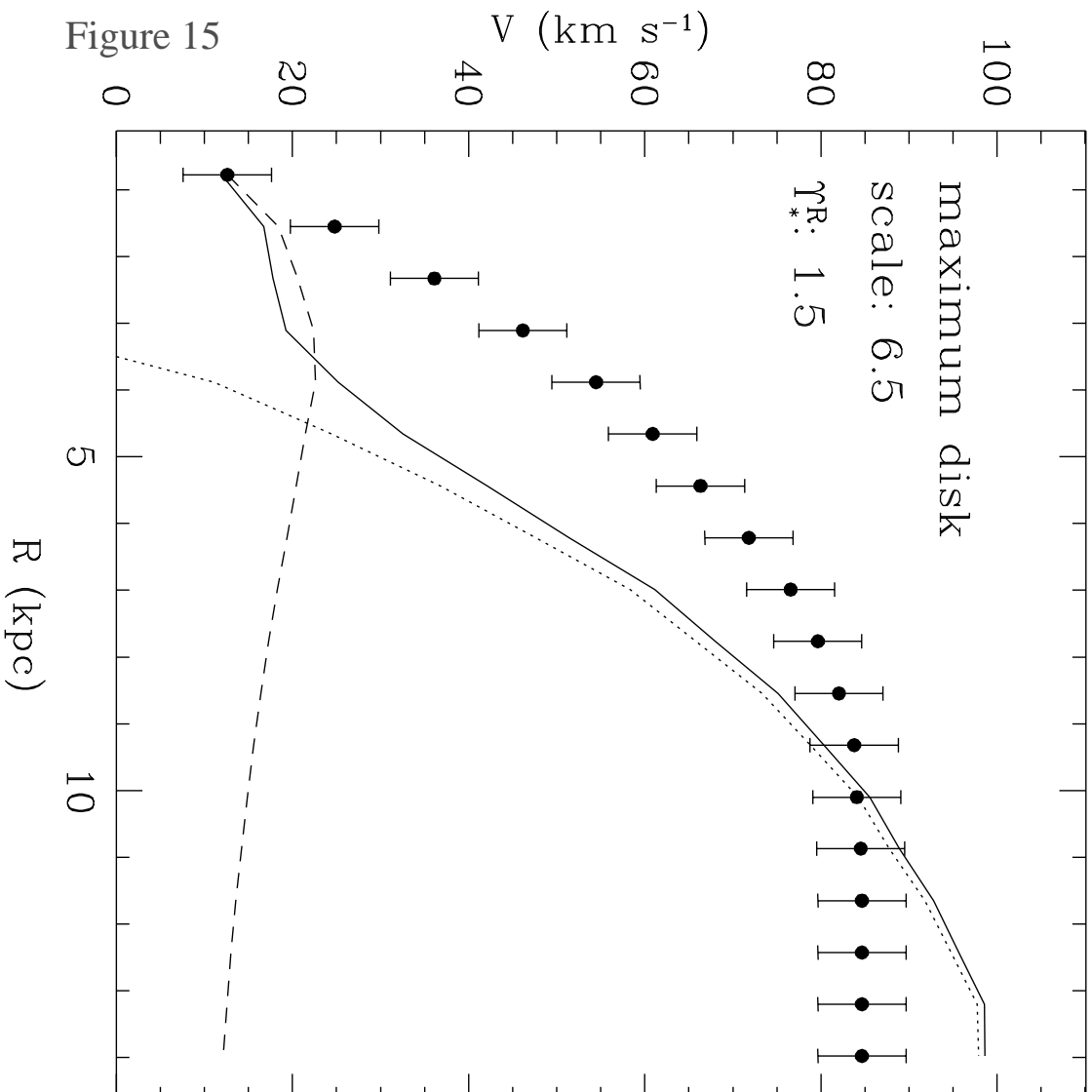


Figure 16

